FBXW7 REGULATION OF NOTCH CONTROLS OLIGODENDROCYTE NUMBER

By

Julia L Snyder

Dissertation

Submitted to the Faculty of the

Graduate School of Vanderbilt University

in partial fulfillment of the requirements

for the degree of

DOCTOR OF PHILOSOPHY

In

Biological Sciences

August 2013

Nashville, Tennessee

Approved:

Bruce Appel, PhD

Charles Singleton, PhD

Kendal Broadie, PhD

Bruce Carter, PhD

Michael Cooper, MD

To my husband, Robert, and daughter, Lauren,

for all their love, support and encouragement

ACKNOWLEDGEMENTS

They say it takes a village to raise a child. I would like to say that it also takes a village to get a PhD. While a PhD is awarded to one person, it would be impossible to do without the support of many, many people.

I would first like to thank my mentor, Dr. Bruce Appel, for allowing me to join his lab and providing the support and guidance throughout my graduate studies. He has influenced as a scientist to think critically of the results of experiments and to present my work in a way to captivate the audience. I would not be where I am today without him.

I would also like to thank my current and former committee members, Dr. Kendal Broadie, Dr. Bruce Carter, Dr. Michael Cooper, Dr. Lilianna Solnica-Krezel, and Dr. Charles Singletary for helpful suggestions and encouragement during committee meetings and preparation of my thesis. The National Institutes of Health Training Program in Developmental Biology grant also financially supported this work.

Success in a lab is also dependent on the members of the lab. They are important for day-to-day communication, as well as in analysis and perspective of results of experiments. All current and former members of the Appel lab were a tremendous help in keeping me motivated and suggesting experiments to help improve my results. We also had a group of zebrafish labs at Vanderbilt that met on a weekly basis whose discussion contributed as well to my project.

Last, but certainly not least, I must thank my family and friends for their support. I would like to thank my husband, Robert, for sticking with me through it all and believing in me when I didn't always believe in myself. I am forever grateful for his patience with me to finish. Also, my parents, Bill and Ceci Porter for allowing me to spread my wings and go to a university several states from home and then supporting me when I decided to change my major and pursue a biology degree. My sister, Sarah, for her love and support. I am also very appreciative of the encouragement from all my friends, both those I knew before graduate school and those I met at graduate school. Your faith and belief in me has helped me to reach this goal. Thank you everyone!

TABLE OF CONTENTS

LIST OF FIGURES

LIST OF ABBREVIATIONS

bHLH	basic Helix-Loop-Helix
BMP	Bone Morphogenic Protein
BrdU	5-bromo-2′-deoxyuridine
BSA	Bulked Segregant Analysis
CNS	Central Nervous System
CPD	Cdc4 phospho-degron
DAPT	N-[N-(3,5-Difluorophenacetyl)-L-alanyl]-S-phenylglycine t-butyl ester
DMSO	Dimethyl sulfoxide
dpf	days post fertilization
DSL	Delta-Serrate-Lag1
ENU	*N*-ethyl *N*-nitrosourea
EST	Expressed Sequence Tag
Fbxw7	F-box protein, WD40 containing 7
FGF2	Fibroblast Growth Factor 2
GSK3-β	Glycogen synthase kinase 3-beta
hpf	hours post fertilization
IGF1	Insulin Growth Factor 1
ILK	Integrin-linked Kinase
Isl	Islet 1/2
JXP	Juxtaparanode
MB1	Myc Box 1

MBP	Myelin Basic Protein
MOG	Myelin Oligodendrocyte Glycoprotein
MPZ (P0)	Myelin Protein Zero
MRF	Myelin Gene Regulatory Factor
MS	Multiple Sclerosis
mTOR	mammalian Target of Rapamyin
NICD	Notch-intracellular Domain
NLS	Nuclear Localization Signal
Node	Node of Ranvier
OPC	Oligodendrocyte Progenitor Cell
PDGF-A	Platelet-Derived Growth Factor A
PDGFR-α	Platelet-Derived Growth Factor Receptor alpha
PLP1a	Proteolipid Protein 1a
PMD	Pelizaeus-Merzbacher Disease
pMN	precursor Motor Neuron
PN	Paranode
RFLP	Restriction Fragment Length Polymorphism
Shh	Sonic hedgehog
SSLP	Simple Sequence Length Polymorphism
TAD	Transactivation Domain
TALEN	TAL-effector nuclease
ZFN	Zinc-finger nuclease

CHAPTER I

INTRODUCTION

The nervous system is a complex organization of classes of neurons and glia that can be broken into a central component (CNS) and peripheral component (PNS). Integration of the CNS and PNS regulates many processes within a body, from movement of muscles to recognition of sensory stimuli. Connection between the CNS and PNS occurs via axons extending from neurons. Information is transmitted along axons in the form of action potentials: current that flows due to depolarization of the plasma membrane. Propagation of action potentials occurs by saltatory, or jumping, conduction due to the presence of myelin on the axon (Bunge, 1968; Baumann and Pham-Dinh, 2001). Sodium (Na^+) channels cluster at nodes of Ranvier, regions where two myelin sheaths abut each other along the axon, and allow the influx of Na^+ ions that depolarize the membrane (Sherman and Brophy, 2005). The depolarization propagates along the length of the axon to the terminal that contacts the next neuron in the circuit (Bean, 2007)

Myelin is a multi-layered structure composed of compacted lipid rich membranes produced by glial cells in the CNS and PNS (Baumann and Pham-Dinh, 2001). Oligodendrocytes in the CNS and Schwann cells in the PNS form myelin by extensions of plasma membrane which wrap around and ensheath

axons (Bunge, 1968; Pfeiffer et al., 1993). A single oligodendrocyte can wrap multiple axons multiple times (Figure 1A) (Pfeiffer et al., 1993), while a single Schwann cell interacts with axons at a one-to-one ratio. Each myelin sheath can be divided into three regions bounded by nodes of Ranvier (Figure 1B) (Baumann and Pham-Dinh, 2001). As the membrane wraps around axons the ends loop down to form the paranode that separates the node from the internode, or interior of the myelin. The loops are connected to each other by adherens junctions and to axons by tight junctions (Salzer et al., 2008). Between the paranode and internode lies the juxtaparanode region. Within the juxtaparanode lie potassium (K^+) channels that are thought to play a role in the resting potential of the internode and prevent excitation from the node spreading into the internode to keep the flow of the signal down the axon (Salzer et al., 2008).

Oligodendrocytes and disease

The importance of myelination, and hence oligodendrocytes, is demonstrated by diseases that alter development or maintenance of the myelin sheath and oligodendrocytes. Developmental diseases of oligodendrocytes are referred to as leukodystrophies. Later in adulthood, diseases such as multiple sclerosis (MS) or injury to the CNS are responsible for demyelination.

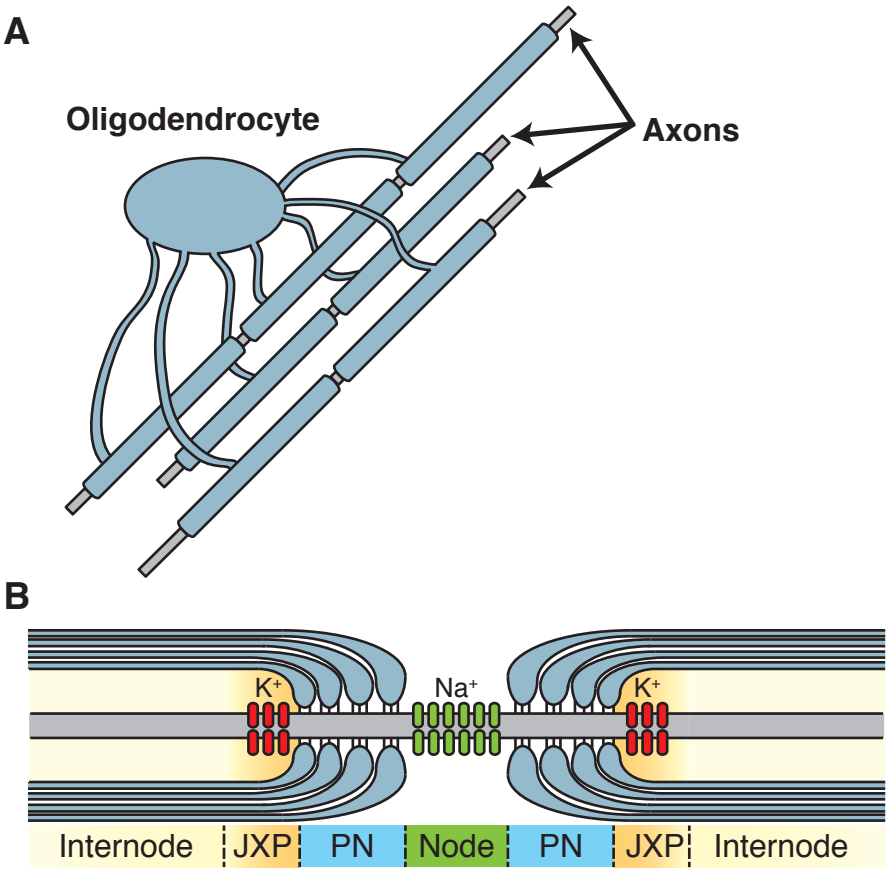

Figure 1 Schematic of oligodendrocyte and myelin regions. (A) Graphic representation of a single oligodendrocyte wrapping several axons with myelin segments. **(B)** Cross-section of adjoining myeling sections showing regions and channel types associated with each. JXP = juxtaparanode, PN = paranode, Node = Node of Ranvier, K^+ = potassium channels, and Na^+ = sodium channels.

Leukodystrophies

Leukodystrophies are a group of inherited disorders characterized by impairment of the growth or maintenance of myelin in the CNS, for example the X-linked disease Pelizaeus-Merzbacher disease (PMD) caused by mutation or duplication of the proteolipid protein (PLP) locus and Krabbe disease caused by mutation of galactocerebroside β galacosidase (GALC) that is required for galactolipid metabolism in myelin (reviewed in (Perlman and Mar, 2012). Most have early onsets in infancy or childhood, although some do have incidences of later onset that are typically less severe. Common symptoms include problems with movement, speech, hearing, vision, and behavior (Lyon et al., 2006; Costello et al., 2009).

PMD symptoms include hypomyelination, problems with movement, feeding, and possibly seizures depending on the severity of the disease (Hobson and Garbern, 2012). Treatments include medications, physical therapy, and surgery. There is currently no cure for PMD.

Krabbe disease is a demyelinating disorder with incomplete metabolism of galactocerebroside due to mutations of GALC. There are two infantile onset forms: early (prior to 6 months of age) and late (6 months to 4 years of age) (Wenger et.al 2012; (Pastores, 2009). Most cases are of the early infantile form, however there are also juvenile and adult-onset forms (Pastores, 2009; Perlman and Mar, 2012). There is also no cure for Krabbe disease.

Demyelinating Diseases

Diseases, such as MS or the peripheral myelin disease Charcot-Marie-Tooth, or CNS injury can lead to demyelination of axons. Loss of myelin affects the ability of axons to efficiently conduct nerve impulses. MS is an inflammatory demyelinating disease that is believed to be autoimmune in nature. MS can be divided into two classes: secondary progressive, which begins with episodes of relapsing and remitting symptoms followed by increasing disability and primary progressive, which is an accumulation of disability with no remission (Lucchinetti et al., 2005). Failure of remyelination in MS could be due to recruitment or differentiation of oligodendrocytes (Franklin, 2002; John et al., 2002). However, recruitment of OPCs to lesions does not appear to contribute to lack of remyelination because lesions have cells that express markers of OPCs (Wood and Bunge, 1991; Blakemore and Keirstead, 1999; Franklin, 1999). As the disease progresses, the ability of these cells to differentiate appears to decrease for reasons that have yet to be elucidated (Wolswijk, 2000; 2002; Kuhlmann et al., 2008). The mechanisms regulating initial remyelination and progressive failure of remyelination are not clear. Understanding the mechanisms used during development could be applied to promote more efficient remyelination.

Development of oligodendrocytes

Oligodendrocytes arise from discrete regions of the brain and spinal cord then migrate to occupy axon tracts, also called the white matter due to the color

of the region after fixation. During development, the number of oligodendrocytes is regulated to ensure that they correlate to the axons that need to be wrapped (Barres and Raff, 1994; Calver et al., 1998). However, the mechanisms that regulate OPC specification and instruct oligodendrocytes to wrap particular axons are unclear.

Spinal cord patterning

Dorsoventral patterning of the vertebrate spinal cord is based on the opposing concentration gradients of two morphogens: sonic hedgehog (Shh) ventrally and bone morphogenic protein (BMP) dorsally. Ectopic placement of notochords in chick and *Xenopus* induced ventral cells types, such as floor plate cells and motor neurons, in the spinal cord adjacent to the ectopic notochord (van Straaten et al., 1988; Clarke et al., 1991; Yamada et al., 1991). This suggested the notochord produces a signal that is necessary for the generation of ventral spinal cord cells. However, the signaling molecule remained unknown. Shh was identified as a homolog of the Drosophila segment polarity *hedgehog* (*hh*) gene in mammals and zebrafish (Echelard et al., 1993; Roelink et al., 1994). Based on sequence homology to the Drosophila *hh* gene, Shh was predicted to be a secreted protein (Echelard et al., 1993) which raised the possibility it could act on cells away from its origin. Additionally, expression of Shh was observed along the ventral midline and in the notochord and floor plate (Echelard et al., 1993) suggesting a possible role in ventral precursor specification. Neural explants

cultured with cells expressing Shh induced floor plate and motor neurons in a dose-dependent manner (Roelink et al., 1994). Further, placement of Shh-secreting cells near neural plate explants of chick explants induced floor plate cells and motor neurons (Roelink et al., 1995). Together, these experiments demonstrate the notochord secretes Shh to pattern the ventral neural tube.

Ventral precursor domains along the dorsoventral axis are established due to the expression of homeodomain transcription factors such as *nkx2.2, nkx6.1* and *nkx6.2*, and the basic helix-loop-helix (bHLH) gene *olig2* by graded Shh activity (Roelink et al., 1995; Briscoe et al., 1999; 2000; Lu et al., 2000; Zhou et al., 2000; Park et al., 2002). Cross-repression of these transcription factors restricts the boundaries between the ventral domains and subsequent classes of neurons and glia that arise from each (Jessell, 2000). Oligodendrocytes arise from the restricted ventral precursor motor neuron, pMN, domain in the vertebrate spinal cord of *Xenopus*, chick, zebrafish, mouse and rat (Figure 2A) (Warf et al., 1991; Pringle and Richardson, 1993; Maier and Miller, 1995; ONO et al., 1995; Park et al., 2002) that also produces motor neurons. Recent evidence also points to a dorsal origin of oligodendrocytes (Fogarty et al., 2005; Vallstedt et al., 2005; Kessaris et al., 2006). Markers of oligodendrocytes were observed when the ventral contribution was eliminated due to loss of the pMN domain (Richardson et al., 2006). Additionally, these oligodendrocytes also expressed markers of dorsal progenitor cells (Fogarty et al., 2005; Vallstedt et al., 2005).

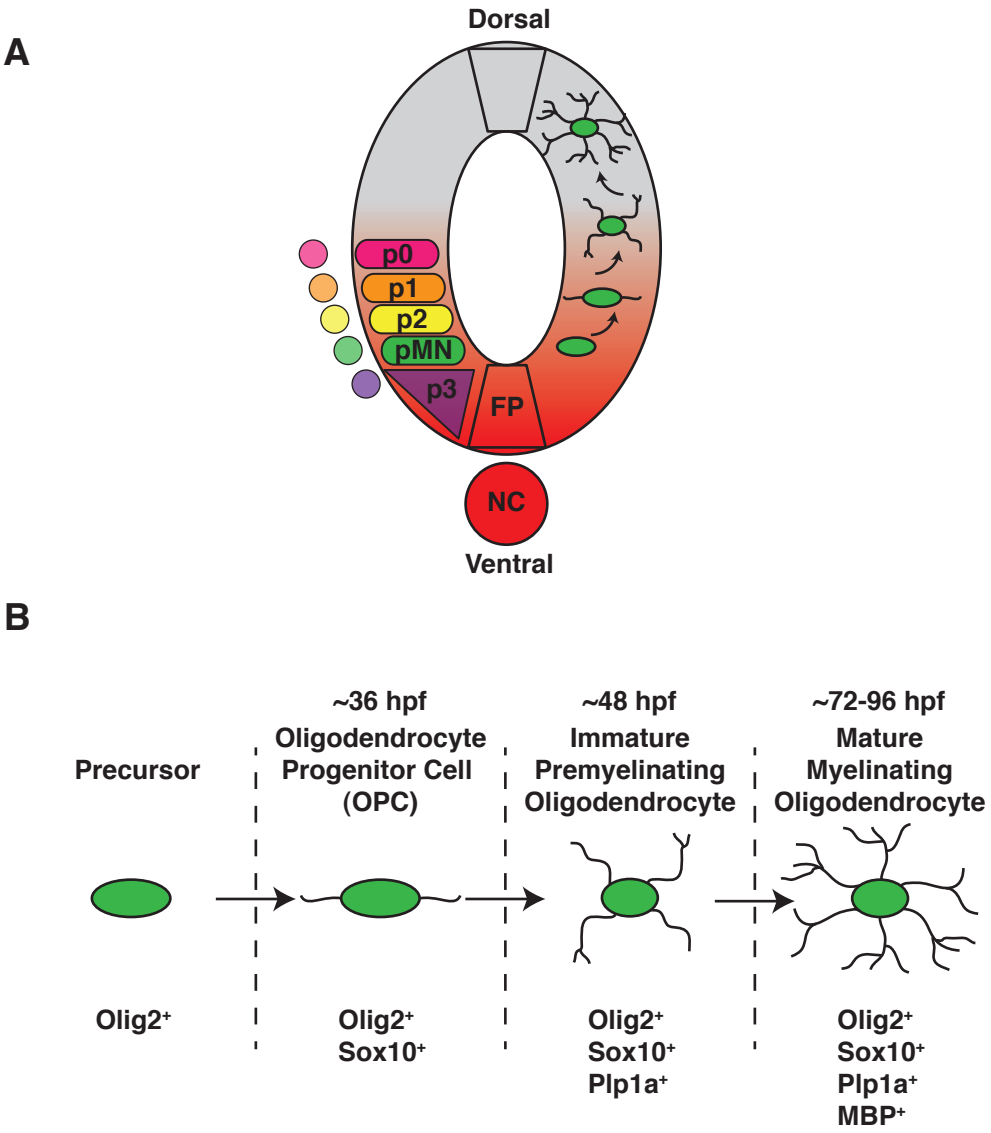

Figure 2 Overview of spinal cord patterning and oligodendrocyte development. (A) Transverse section of a spinal cord with the ventral domains indicated on left and stages of oligodendrocyte development on right. Red represents gradient of Shh expression. Grey represents gradient of BMP expression. **(B)** Stages of oligodendrocyte development showing changes in process formation and expression of different markers along the lineage, as well as approximate timing in zebrafish.

Groups seeking to find early markers of oligodendrocytes identified the Olig genes. Based on the knowledge that several bHLH transcription factors such as Neurogenin and NeuroD are critical for motor neuron specification (Lee et al., 1995; Ma et al., 1996; Sommer et al., 1996), it was hypothesized that novel bHLH transcription factors would also be required for oligodendrocyte development. Two bHLH genes, Olig1 and Olig2, were identified and found to be expressed in oligodendrocytes (Lu et al., 2000; Takebayashi et al., 2000; Zhou et al., 2000). Expression of *Olig2* preceeded the earliest oligodendrocyte markers, raising the possibility it could also be a marker of pMN precursors (Lu et al., 2000; Takebayashi et al., 2000). Indeed, double mutants lacking both *Olig1* and *Olig2* lose oligodendrocytes and generate V2 interneurons in place of mototneurons (Zhou and Anderson, 2002). Further support comes from induction of motor neuron markers by misexpression of *Olig2* in chick (Novitch et al., 2001).

Oligodendrocyte lineage progression

Oligodendrocytes proceed through a differentiation process marked by the appearance of receptors, transcription factors and myelin proteins at distinct times, starting as specified oligodendrocyte progenitor cells (OPCs) and continuing through to mature oligodendrocytes with compact myelin.

Prior to the initial specification of OPCs, precursors within the pMN domain must undergo a switch from neurogenesis to oligodendrogenesis. Expression of Ngn1 and Ngn2 in pMN precursors during neurogenesis suggests OPC

specification is inhibited by Ngns (Zhou et al., 2001). Alternatively, Sox9, NFIA, and NFIB expression is initiated in precursors prior to gliogenesis and are required for timing of oligodendrogenesis (Stolt et al., 2003; Deneen et al., 2006), indicating they influence the switch.

Initial specification markers of oligodendrocytes include platelet-derived growth factor receptor α (PDGFRα) and the HMG-box transcription factor Sox10. Addition of the ligand platelet-derived growth factor A (PDGF-A) to cells isolated from the optic nerve induced formation of oligodendrocytes (Raff et al., 1988). PDGFRα expression in oligodendrocytes was first demonstrated in cultures of O-2A cells (a cell type that gives rise to both oligodendrocytes and type-2 astrocytes *in vitro*) purified from the cerebral hemispheres of rat brain (McKinnon et al., 1990). Additionally, overexpression of the PDGF-AA ligand produced an excess of OPCs as indicated by labeling for PDGFRα (Calver et al., 1998). However, zebrafish do not express *pdgfrα* or *pdgf-a* in the spinal cord, indicating that oligodendrocytes in zebrafish do not require this pathway to produce oligodendrocytes (Liu et al., 2002a; 2002b).

Sox10 expression precedes that of PDGFRα and is maintained throughout differentiation of the oligodendrocyte lineage (Figure 2B) (Kuhlbrodt et al., 1998). However, loss of Sox10 does not alter specification of oligodendrocytes as demonstrated by LacZ knock-in to the Sox10 locus in mice and the *colorless* (*cls*) mutant in zebrafish. Nevertheless, both produce deficits in differentiation and

myelination (Stolt, 2002; Takada and Appel, 2010) suggesting Sox10 is required for progression of the lineage.

Following specification, OPCs divide and migrate to occupy the spinal cord. During this immature stage, cells have a characteristic bipolar morphology (Pfeiffer et al., 1993; McMorris and McKinnon, 1996). Timelapse imaging of zebrafish embryos reveals dynamic process extension and retraction as OPCs migrate (Kirby et al., 2006). Contact with processes from neighboring cells induces retraction and appears to space OPCs along axons and relative to each other (Kirby et al., 2006). Expression of *proteolipid protein 1a* (*plp1a*) begins during this stage (Figure 2B). Loss of *plp* in the naturally-occurring mutants *jimpy* and *rumpshaker* leads to hypomyelination (Griffiths et al., 1990; Fanarraga et al., 1992). An interesting observation in the *rumpshaker* mutants is an increase in oligodendrocyte number in the spinal cord at postnatal day 16. This suggests that hypomyelination might induce proliferation of OPCs to compensate for the deficit of myelin in these mutants (Fanarraga et al., 1992).

As immature oligodendrocytes become post-mitotic and wrap axons they begin to express genes specific to myelin, such as *mbp* and *myelin protein zero* (*mpz* or P0) (Figure 2B). Loss of these genes results in defects of the myelin sheath as demonstrated by the shiverer mouse, which has a mutation within *Mbp* (Brady et al., 1999) and leads to dysmyelination of axons. Expression of *mbp* is regulated by Sox10 (Stolt, 2002)

Myelin gene regulatory factor (MRF) is a recently identified transcription factor required for expression of myelin genes. *Mrf* was identified in a transcriptome analysis of postmitotic oligodendrocytes from postnatal mouse forebrain (Cahoy et al., 2008; Emery et al., 2009). Knockdown of *Mrf* with small-interfering RNAs (siRNAs) in oligodendrocyte cultures or conditional knockout of a floxed *mrf* allele by *olig2* driven Cre resulted in a decrease in the expression of the myelin genes *mbp* (*myelin basic protein*) and *mog* (*myelin oligodendrocyte glycoprotein*). Overexpression of *Mrf* in mouse OPCs *in vitro* and *in vivo* electroporation of chick embryos resulted in increased expression of MBP and MOG (Emery et al., 2009).

Notch

While many of the steps of oligodendrocyte differentiation are marked by expression of various transcription factors and myelin proteins, the mechanisms that regulate the process are not well understood. One pathway known to play a role in oligodendrocyte development is the Notch signaling pathway (Park and Appel, 2003; Park et al., 2005; Thomas and van Meyel, 2006; Shin et al., 2007; Taylor et al., 2007; Rabadán et al., 2012).

Identification of Notch first came from studies of the *Drosophilia* wing disc nearly a century ago by TH Morgan and colleagues. The Notch locus is situated on the X-chromosome and the mutation Morgan studied was a small deletion including Notch (Dexter, 1914; Mohr, 1919). Heterozygous female flies with this Notch mutation display a notch in the wing disc, while homozygous females and

hemizygous males are embryonic lethal indicating a dominant, halploinsufficient, X-linked allele. Although the chromosomal region was known for some time, the links between gene, protein, and function were not understood. Cloning of Notch revealed a receptor important for signaling between cells (Artavanis-Tsakonas et al., 1983; Kidd et al., 1983; Tsakonas and Grimwade, 1983). Identification of homologs in *C. elegans* and *Xenopus* followed (Greenwald et al., 1983; Austin and Kimble, 1987; Greenwald, 1987; Priess et al., 1987; Coffman et al., 1990).

Notch signaling pathway

The Notch signaling pathway consists of a transmembrane receptor on a signal-receiving cell that binds to a transmembrane ligand on a neighboring signal-sending cell (Figure 3). Mammals possess four Notch receptors (Notch 1-4) and a total of 5 ligands from the DSL (Delta-Serrate-Lag1) family: Delta-like 1, 3 and 4 and Jagged (Serrate-like) 1 and 2. After ligand binding, the Notch receptor undergoes two proteolytic cleavages to produce the Notch-intracellular domain (NICD). First ADAM-family metalloproteases (Wen et al., 1997; van Tetering et al., 2009) cleave the Notch receptor at the S2 site within the membrane followed by a γ-secretase complex (Fortini, 2002; Selkoe and Kopan, 2003) NICD then translocates to the nucleus and interacts with the co-activator RBP-Jκ to activate downstream targets, notably members of the Hes transcription factor family (Schroeter et al., 1998; Castro, 2005) and reviewed in (Borggrefe and Oswald, 2009)).

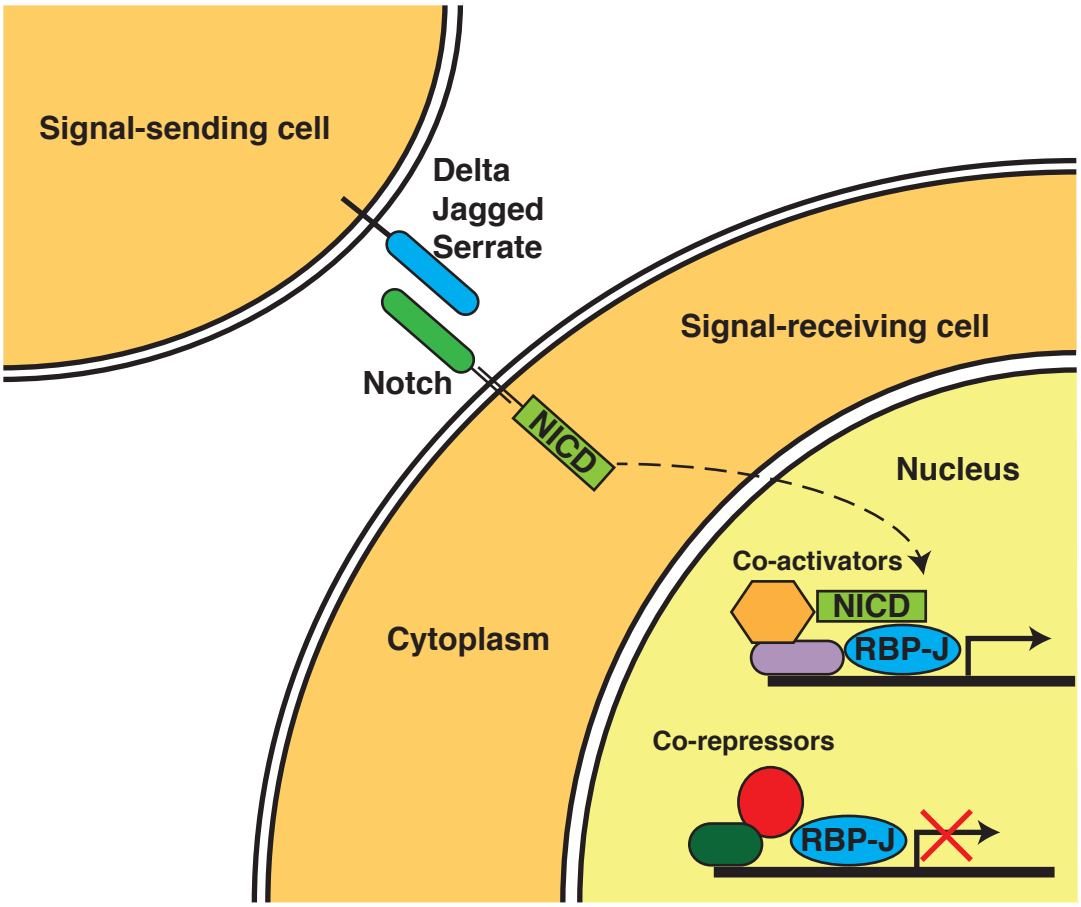

Figure 3 Overview of Notch signaling pathway. Neighboring cells send and receive signals via membrane-associated ligands and receptors. The signal-sending cell expresses a ligand (Delta, Jagged, or Serrate) while the signal-receiving cell expresses a Notch receptor. Activation of the Notch receptor by a ligand produces a proteolytic cleavage of the receptor releasing the intracellular domain (NICD). NICD then translocates to the nucleus to complex with co-activators and induce transcription of downstream target genes.

Notch signaling is most commonly associated with a process termed lateral inhibition by which one cell inhibits a neighboring cell from acquiring the same fate as itself (Artavanis-Tsakonas et al., 1999). Typically one cell will differentiate while the other remains in an undifferentiated state. Another possible result of Notch signaling is a cell fate decision. In the spinal cord for example, cells from the p2 domain produce two different types of interneurons (V2a or V2b) in response to Notch activity (Kimura et al., 2008). Activation of Notch signaling produces V2b interneurons while inhibition produces V2a (Del Barrio et al., 2007).

Another example of cell fate specification by Notch in the spinal cord is the production of neurons and glia. Loss of Notch signaling results in increased neurogenesis at the expense of glia, including oligodendrocytes, due to failure of neural precursor maintenance (Chitnis et al., 1995; de la et al., 1997; Appel and Eisen, 1998; Appel et al., 2001; Lütolf et al., 2002; Itoh et al., 2003; Park and Appel, 2003; Imayoshi et al., 2010), and elevated expression of the proneural genes *Ngn1* and *Ngn2* (Yang et al., 2006). If loss of function of Notch signaling leads to deficits of OPCs, gain of function would be expected increase OPCs at the expense of motor neurons. Consistent with this hypothesis, global induction of a constitutively active form of NICD in zebrafish leads to decreased neurogenesis and a two-fold increase in oligodendrocytes (Park and Appel, 2003). However, formation of the excess OPCs appeared to come from pMN precursors, indicating other factors are required (Park and Appel, 2003).

Post-translational modifications of the Notch receptor

Notch is comprised of several domains important to function. The extracellular region contains epidermal-like growth factor (EGF) and LIN repeats which can be post-translationally modified, while the intracellular regions contains a RAM domain, ankyrin repeats and a PEST domain. As Notch is synthesized in the endoplasmic reticulum (ER) it undergoes post-translation modifications of the extracellular regions and cleavage of the S1 (site1) by furin. Notch receptor is then translocated to the cell membrane as a heterodimer (reviewed in (Michailov et al., 2004; Fortini, 2009)).

Notch signaling must be regulated to ensure that cells acquire the appropriate fate for the tissue (Bray, 2006; Andersson et al., 2011). One mechanism to regulate signaling is through the ligands. Signaling between the ligand and receptor can happen either in *trans* (between two different cells) or *cis* (within the same cell) (Sprinzak et al., 2010). Typically *cis* interactions inhibit Notch, while *trans* interactions activate Notch. Investigation of photoreceptor specification in the fly eye demonstrated that mosaic mutation of Delta results in fate transformation only in mutant cells (Miller et al., 2009). These results indicate Delta expression in wildtype cells is able to regulate Notch signaling by cis-interactions. Two possible mechanisms for *cis*-inhibition are 1) during trafficking to the cellular membrane or 2) once Notch reaches the cell surface. Interactions of the Notch receptor with *cis* or *trans* ligands are thought to regulate and fine-tune the level of signaling in a cell (Rowitch and Kriegstein, 2010; Sprinzak et al., 2010).

Ubiquitin ligases

Another mechanism for regulating protein activity is through protein degradation by the proteosome. During development, it is critical that factors for a given stage be regulated such that they are only available to exert their effect at the proper time. The question arises as to how a cell knows to degrade a particular protein. Signaling within a cell produces many modifications to proteins that influence downstream effectors, including ubiquitination. Ubiqiuitin is a small peptide covalently attached to the protein sometimes as a single unit and at other times in long chains. The degree of ubiquitination determines the cell's response to proteins. Proteins with multiple ubiquitin molecules, polyubiquitination, are degraded by the 26S proteosome. The most well characterized role for the ubiquitin proteasome system is in cell cycle control (Glotzer et al., 1991) and reviewed in (Nakayama and Nakayama, 2006).

Addition of ubiquitin to proteins requires a series of enzymes: E1s are ubiquitin-activating; E2s conjugate ubiquitin and mediate the transfer to substrates via E3 ubiquitin ligases, the substrate recognition component of the complex (Fang and Weissman, 2004; Parpura et al., 2012). Four main families of E3s are classified by the following structural motifs: HECT domain, RING-finger domain, U-box domain or PHD-finger domain. The largest family is the RING-finger domain containing, which is further subdivided into classes that contain one of seven different Cullins (reviewed in (Fang and Weissman, 2004; Ishibashi et al., 2006)). The most common cullin-based E3s are the Anaphase Promoting Complex/Cyclosome (APC/C) and SCF (Skp1/Cul1/F-box-protein).

APC/C and SCF E3 ligase complexes

As might be suggested by the name, APC/C regulates the transition from metaphase to anaphase during mitosis as well as cell cycle exit by targeting proteins involved in the cell cycle. APC/C is a complex of 13 different proteins, including Apc1 (cullin subunit) and Apc11 (RING-finger domain containing). Much research is currently being done to understand the role of the additional proteins in the complex (reviewed in (Peters, 2006; Saijo and Glass, 2011)).

SCF complexes on the other hand are active from G1 until entry to mitosis and comprised of 3 invariable subunits: Skp1 (adaptor protein), Cul1 (cullin subunit), Rbx1 (RING-domain containing), plus the variable F-box protein (Fbx) which is the substrate recognition subunit. Skp1 binds to the F-box domain of Fbx proteins to bring the substrate in close proximity to the complex for transfer of ubiquitin.

F-box protein family

Fbx proteins contain a common amino-terminal F-box domain, which is required for binding to the E3 complex, as well as a C-terminal motif critical for substrate recognition. Fbx proteins are classified based on their C-terminal motifs: FBXLs contain Leucine-Rich Repeats (LRRs), FBXWs contain WD40 repeats, and FBXO contain either a different or no motif. WD40 repeats in Fbxw proteins form β-propeller sheets that fold to generate a binding pocket for the substrate.

Fbxw7 was first identified as Cdc4 in a screen in yeast looking for cell cycle effectors (Hereford and Hartwell, 1974; Prinz et al., 2011). A screen in *C. elegans* for suppressors of a partial loss of function of the Notch homologue LIN-12 discovered Sel-10 as a negative regulator of *lin-12* (ref). Further characterization in *C. elegans* determined *sel-10* is a homologue of *cdc4* (Hubbard et al., 1997; Salzer et al., 2008). The mammalian homologue was found by looking for F-box proteins that could bind specifically to CyclinE using tissue culture (Strohmaier et al., 2001; Salzer et al., 2008) and through identification of the mouse homologue (van Straaten et al., 1988; Clarke et al., 1991; Yamada et al., 1991; Maruyama, 2001). In addition to the F-box and WD repeat domains, Fbxw7 also contains a dimerization domain thought to be important for increased binding efficiency to suboptimal substrates (Roelink et al., 1995; Welcker and Clurman, 2007).

By using the yeast target Sic1, Nash et. al delineated the Cdc4-phospho-degron (CPD) motif with the following consensus sequence: I/L–I/L/P–pT–P–<K/R>4, where <X> indicates unfavorable residues (Roelink et al., 1995; Briscoe et al., 1999; 2000; Nash et al., 2001). Sic1 contains nine suboptimal motifs, of which six must be phosphorylated for Cdc4(Fbxw7) recognition (Warf et al., 1991; Pringle and Richardson, 1993; Maier and Miller, 1995; ONO et al., 1995; Nash et al., 2001; Park et al., 2002). Mutations of the CPDs result in disruption of Fbxw7 binding and substrate stabilization (reviewed in (Rowitch, 2004; Welcker and Clurman, 2008)).

Mammals possess three isoforms of Fbxw7: α, β, and γ. Each of which contains a unique 5' exon joined to a common set of exons (Spruck et al., 2002; Liu et al., 2002a; 2002b). Each isoform contains its own promoter to generate isoform-specific transcripts that results in tissue-specific expression of each isoform. Fbxw7-α is ubiquitously expressed, Fbxw7-β is enriched in the CNS, and Fbxw7γ is higher in muscle (Raff et al., 1988; Matsumoto et al., 2006). An additional level of complexity comes from the dimerization capacity of Fbxw7 that allows for degradation of suboptimal phosphorylation of targets (Welcker and Clurman, 2007).

Fbxw7 targets

Cyclin E is the most well characterized target of Fbxw7 and regulates the transition from the G1 phase to S phase in mitotically cycling cells. Misregulation of Cyclin E can allow a cell enter S phase before the cell is ready, if DNA damage needs to be repaired, for example. Premature entry into S-phase leads to aberrant mitosis and misappropriation of chromosomes and chromosomal instability.

Notch signaling results in the release of NICD that translocates to the nucleus to activate gene transcription. Characterization of NICD determined the carboxy-terminal PEST domain contains the CPD required for degradation by Fbxw7 (Calver et al., 1998; Oberg, 2001; Fryer et al., 2004). Knockout mice for *fbxw7* die *in utero* due to defects in hematopoiesis and vascularization, both of

which are known to require Notch signaling (Lee et al., 1995; Ma et al., 1996; Sommer et al., 1996; Tetzlaff et al., 2004; Tsunematsu, 2004).

Identification of c-Myc as a target of Fbxw7 came from a study that investigated one of two sites known to be important for c-Myc stability and frequently mutated in cancers, MB1 (Myc box 1) (Lu et al., 2000; Takebayashi et al., 2000; Zhou et al., 2000; Yada et al., 2004). Further characterization of the interaction between c-Myc and Fbxw7 revealed each isoform had different subcellular localizations that determined target degradation based on dominant signals within the unique first exon. Fbxw7α contains a nuclear localization signal (NLS), Fbxw7β possess a hydrophobic transmembrane domain, and Fbxw7γ does not contain a dominant signal and localizes to the nucleolus due to a signal in the common region. For example, targeting of c-Myc was shown to occur in the nucleolus (Novitch et al., 2001; Welcker et al., 2004) and also in the nucleus (Popov et al., 2007; Hueber and Lohmann, 2008).

Mao et al. (Mao et al., 2008; Tümpel et al., 2009) used the consensus CPD sequence to scan a mouse protein database for novel targets of Fbxw7. The HEAT domain of mammalian target of rapamycin (mTOR) was pulled out as containing a CPD. Investigation with *Fbxw7*$^{-/-}$ mouse embryonic fibroblasts (MEFs) revealed increased levels of mTOR as well as phosphorylated mTOR with no change in upstream signaling. Additionally, ubquitination of mTOR was found only in cells with functional Fbxw7. Differentiation of oligodendrocytes has been shown to be regulated by mTOR (Narayanan et al., 2009; Gotoh et al., 2011).

Role of Fbxw7 in cancer

Mutations in *fbxw7* have been found in various types of cancer, including blood, bile duct, breast, colon, endrometrium, stomach, lung, ovary, pancreas and prostrate (reviewed in (Kuhlbrodt et al., 1998; Akhoondi et al., 2007; Tan et al., 2008). Most of the mutations are missense with hotspots located at the arginine residues critical for substrate recognition and binding. While the overall rate of cancers with *fbxw7* mutations is low, evidence suggests Fbxw7 may be a haploinsufficient tumor suppressor as many other cancers contain deletions of the chromosomal region 4q31.3 that includes the *fbxw7* locus. A study investigating mutations in relation to lung cancer also found a difference between missense mutations and null alleles with regard to embryonic lethality and morphological deficits (Stolt, 2002; Takada and Appel, 2010; Davis et al., 2011).

Support for the halpoinsufficiency of *fbxw7* is exemplified by mice that are doubly heterozygous for mutation of *fbxw7* and *p53*. Double heterozygous mice exhibit increased rates of tumorigenesis after irradiation compared with either wildtype or $p53^{-/-}$ mice. Additionally, the mice developed epithelial tumors that single $p53^{-/-}$ normally do not produce (Mao et al., 2004; Cahoy et al., 2008; Emery et al., 2009).

Altering the activity of signaling pathways, including Notch, or application growth factors, including PDGF-A, modulates OPC number and differentiation. However, the intracellular mechanisms involved in these pathways that influence OPC number remain to be elucidated. We examined the idea that the excess OPCs formed in the zebrafish mutant *vu56* arise due to misregulation of Notch

activity. The work presented here demonstrates Fbxw7 regulation of Notch signaling is one aspect that controls oligodendrocyte number.

CHAPTER II

METHODS

Zebrafish husbandry

Embryos were produced by pair wise matings, raised at 28.5°C in egg water or embryo medium (EM), and staged to hours post-fertilization (hpf) or days post-fertilization (dpf) as previously described (Kimmel et al., 1995; Emery et al., 2009). Zebrafish strains used include: AB, *Tg*(*olig2:EGFP*) (Brady et al., 1999; Shin et al., 2003), *Tg*(*Tp1bglob:hmgb1-mCherry*)^{jh11} (Griffiths et al., 1990; Fanarraga et al., 1992; Parsons et al., 2009) and *fbxw7*^{vu56}.

Mutant screen

The *vu56* allele was identified in a screen for mutations that altered the number and distribution of OPCs, revealed by *Tg(olig2:EGFP)* reporter expression. AB males were mutagenized with *N*-ethyl *N*-nitrosourea (ENU) as described previously (Solnica-Krezel et al., 1994; Hobson and Garbern, 2012). Mutagenized males were crossed to *Tg(olig2:EGFP)* females to create an F1 generation. F1 fish were raised to adulthood and crossed to wild-type *Tg(olig2:egfp)* fish to create F2 families. F2 siblings were randomly intercrossed and their progeny screened using fluorescent stereomicroscopes. Identified F2 *vu56* heterozygotes were outcrossed to AB fish to propagate the line and to the WIK laboratory strain to create families for genetic mapping. The *vu56* allele has been maintained by repeated outcrossing to AB fish.

Immunohistochemistry

Embryos were fixed using 4% paraformaldehyde, embedded, frozen and sectioned using a cryostat microtome as previously described (Park and Appel, 2003; Lucchinetti et al., 2005). We used the following primary antibodies: rabbit anti-Sox10 (1:500) (Franklin, 2002; John et al., 2002; Park et al., 2005), mouse anti-Isl (39.4D5, Developmental Studies Hybridoma Bank (DSHB) Iowa City, Iowa USA, 1:100), mouse anti-Zn8 (1:1000, DSHB), mouse anti-Hu (1:100, Invitrogen) and mouse anti-Zrf1 (1:250, DSHB). For fluorescent detection of antibody labeling, we used Alexa Fluor 568 goat anti-mouse or goat anti-rabbit conjugates (Invitrogen, 1:200). Images were captured using either a Zeiss Axiovert 200 inverted microscope equipped with a PerkinElmer Ultraview ERS Live Cell Imager spinning disc confocal system or a Zeiss AxioObserver inverted microscope equipped with a PerkinElmer Ultra*VIEW* VoX confocal system and analyzed with Volocity software (PerkinElmer) and Adobe Photoshop. Image adjustments were limited to contrast enhancement, level settings, auto tone and cropping.

Mapping and PCR genotyping

fbxw7^{vu56} mutants were identified at 3 dpf and collected with wild-type siblings for isolation of DNA in lysis buffer (10 mM Tris pH 8.0, 50 mM KCl, 0.3% Tween-20, 0.3% NP-40) with 1 µg/µL Proteinase K at 55°C overnight. Pooled DNA was used for bulked-segregant analysis (Wood and Bunge, 1991; Postlethwait and

Talbot, 1997; Blakemore and Keirstead, 1999; Franklin, 1999) with published simple sequence length polymorphisms (SSLPs) (www.zfin.org). Individual embryos were used to determine recombination frequencies for finer mapping of *fbxw7*^{vu56}. The following primers were designed to amplify sequences flanking the mutation for restriction fragment length polymorphism genotyping: *fbxw7* forward primer: 5'-CAG TTG ATT TAC CTT TGC GT-3'; reverse primer: 5'-TGT GTC AAT GTG TTT CGG TT-3'. Products were digested with BamHI and HinfI and analyzed using agarose gel electrophoresis.

Isoform cloning and RT-PCR analysis of expression

We obtained clones corresponding to *fbxw7* α, β and γ transcripts using PCR to amplify genomic sequences, which were cloned into pCR2.1-TOPO vectors. The following primer pairs were used for amplification: α, 759 bp product, 5'-CAGAATGCCAAGTCCTTGTC-3'/5'-CCTATTCGGTGAGCGAAGG-3'; β, 254 bp product, 5'-GGCTCAGTCAGTCCGCTCAG-3'/5'-TTTATAGAAGATCATCTTTAAAGTG-3'; γ, 520 bp product, 5'-GCTTGGTGTGAACACTTAAAAC-3'/5'-CATAATTGCATCATTTCCACATT-3'. To investigate expression at different developmental stages we used the isoform specific forward primers with the reverse primer 5'-CGT CGT CTC TGT GGA ACC-3' from the common region to amplify cDNA from single-cell, 24 hpf, and 3 dpf embryos.

In situ RNA hybridization

The following RNA probes were generated: *fbxw7*, which recognizes all isoforms, from an EST (EB835996), *α-fbxw7*, *β-fbxw7*, and *γ-fbxw7* isoform specific probes from 24 hpf cDNA, and *plp1a* and *mbp* (Wolswijk, 2000; Br samle and Halpern, 2002; Wolswijk, 2002; Kuhlmann et al., 2008). *in situ* RNA hybridization was performed according to published methods (Hauptmann and Gerster, 2000; Park and Appel, 2003; Park et al., 2005; Thomas and van Meyel, 2006; Shin et al., 2007; Taylor et al., 2007; Rabadán et al., 2012). Embryos were either mounted for whole-mount imaging or embedded and sectioned as above. Images were captured using either an Olympus AX70 microscope equipped with DIC optics, a Retiga Exi-cooled CCD camera (QImaging) and Openlab software (Improvision) or a similarly equipped Zeiss AxioObserver inverted microscope and Volocity software (Improvision). Image data were exported to Adobe Photoshop and adjustments were limited to level settings, color balance and cropping.

Quantitative PCR

RNA was isolated from 3 sets of 20 pooled wild-type larvae and 3 sets of 20 pooled *fbxw7*$^{-/-}$ larvae at 4 dpf. Reverse Transcriptase was performed using Superscript III First Strand Synthesis for qPCR (Invitrogen). Real-time qPCR was performed on each sample in triplicate using an Applied Biosystems StepOne Plus machine and software version 2.1. Taqman Gene Expression Assays (Applied Biosystems) were used to detect *her4.2* (Dr03160688_g1) and *bactin1* (Dr03432610_m1).

In vivo time-lapse imaging

Embryos were lightly anesthetized using Tricaine, mounted on their sides in 0.7% low-melting temperature agarose in 35 mm glass bottom dishes and covered with EM containing Tricaine. Z-stack images were captured every 15 minutes for 24 hours using an inverted Zeiss AxioObserver equipped with motorized and heated stage and a PerkinElmer Ultra*VIEW* VoX confocal system. The imaging chamber was maintained at 28.5°C. 4D data sets were analyzed using Volocity software (PerkinElmer) and movies were exported to QuickTime. Image adjustments were limited to contrast enhancements and cropping frame size.

Morpholino injections

fbxw7^{SSMO}, consisting of the sequence 5'-GCCAACTACAACAAGACAGAGACAG-3' (Gene Tools, LLC) was designed to have sequence complementary to the boundary of intron 4 and exon 5 of *fbxw7*. The MO was resuspended in sterile water to a stock concentration of 1 mM and stored at room temperature. The stock was diluted in 2X injection buffer (240 mM KCl, 40 mM HEPES, and 0.5% Phenol red) to a concentration of 0.125 mM and 2nL was injected into the yolk of one- to two-cell stage embryos.

DAPT treatments

The γ-secretase inhibitor *N*-[*N*-(3,5-difluoro- phenacetyl-l-alanyl)]-*S*-phenylglycine *t*-butyl ester (DAPT) (Calbiochem) was resuspended in dimethyl sulfoxide (DMSO) to a stock concentration of 20 mM and stored in aliquots at -20°C.

Embryos were manually dechorionated at 36 hpf and placed in 25 μM or 50 μM in EM with 1% DMSO for 12 hours at 28.5°C. DAPT solution was replaced with EM and embryos were allowed to develop to 3 dpf at 28.5°C. At 3 dpf embryos were imaged individually using a stereomicroscope equipped with bright field and epifluorescence optics followed by DNA isolation and *fbxw7*^{vu56} genotyping as described above.

BrdU labeling

Dechorionated embryos were labeled with 5-bromo-2′-deoxyuridine (BrdU) (Roche) by incubating them in 20 mM BrdU in EM with 10% DMSO at room temperature for 30 min. The embryos were then rinsed and maintain at room temperature for 30 min and then fixed using 4% paraformaldehyde. After embedding and sectioning as described above, the tissue sections were treated with 2 N HCl for 30 min before processing for anti-BrdU immunohistochemistry.

Data quantification and statistical analysis

Cell counts were obtained by direct observation of sections using the microscopes described above. For Sox10, *mbp*, and *plp1a* quantification, 10 sections per embryo were counted to produce the average number per section. For Isl quantification, 9 sections per embryo were counted to produce the average number per section. GraphPad Prism software was used for statistical analysis.

CHAPTER III

CHARACTERIZATION OF THE *vu56* MUTATION

Introduction

The central nervous system (CNS) is comprised of a variety of neuronal and glial subtypes. Oligodendrocytes are a glial subtype responsible for producing a specialized plasma membrane termed myelin. During development oligodendrocytes extend processes that wrap axons with myelin, which allows for the saltatory conduction of nerve impulses. Diseases and injuries that disrupt the myelin sheath underscore the importance of this modification.

Oligodendrocyte progenitors were first identified by their expression of platelet-derived growth factor receptor α (PDGFRα) in rat spinal cord (Dexter, 1914; Mohr, 1919; Pringle and Richardson, 1993) and 04 in chick (Artavanis-Tsakonas et al., 1983; Kidd et al., 1983; Tsakonas and Grimwade, 1983; ONO et al., 1995; Miller et al., 1997). Later, the basic helix-loop-helix (bHLH) transcription factors Olig1 and 2 (Greenwald et al., 1983; Austin and Kimble, 1987; Greenwald, 1987; Priess et al., 1987; Coffman et al., 1990; Lu et al., 2000; Takebayashi et al., 2000; Zhou et al., 2000) were identified and used to determine that motor neuron and oligodendrocyte cell fates arise from the ventral pMN domain of the spinal cord (Schroeter et al., 1998; Richardson et al., 2000; Park et al., 2002). However, oligodendrocyte specification is not completely

restricted to the ventral spinal cord as several groups have demonstrated oligodendrogenesis in the dorsal spinal cord. (Cai et al., 2005; Fogarty et al., 2005; Vallstedt et al., 2005; Kessaris et al., 2006; Richardson et al., 2006; Kimura et al., 2008).

Another early marker of specified oligodendrocyte progenitor cells (OPCs) is Sox10, which, in combination with Olig1/2, is reported to regulate expression of the myelin gene *myelin basic protein* (*mbp*) (Irvine, 1999; Stolt, 2002; Li et al., 2007; Liu et al., 2007). In mice, loss of Sox10, in conjunction with loss of Sox9 after specification, leads to apoptosis of OPCs (Finzsch et al., 2008; Oginuma et al., 2010; Niwa et al., 2011). Whereas in the zebrafish, the *colorless* (*cls*) mutant, a nonsense mutation of Sox10, is sufficient to induce apoptosis of OPCs (Takada et al., 2010). Together, these results suggest expression of Sox10 is required for survival and maturation of OPCs.

After specification, OPCs enter a stage described as immature oligodendrocytes where they have a bipolar morphology and are both proliferative and migratory. Immature OPCs migrate to populate the white matter of the CNS. As OPCs proceed through the lineage they begin to express proteins required for myelination, such as *plp1a*, *myelin protein zero*, and *mbp*. Each stage along the differentiation pathway is distinguished by the expression of various transcription factors and myelin components. What remains unknown are the signals that instruct an oligodendrocyte to stop dividing and migrating, wrap axons, and produce myelin-specific proteins.

We used a forward genetic screen to discover novel mechanisms involved in oligodendrocyte development. We identified one mutation, *vu56*, which produced an excess number of OPCs. Positional cloning revealed *fbxw7*, a gene encoding an E3 ubiqutin ligase, was disrupted in *vu56*. Fbxw7 (F-box and WD repeat domain-containing 7) is the substrate recognition component of the SCF (Skp1-Cul1-F-box) E3 ubiquitin ligase complex that targets proteins for degradation (Welcker and Clurman, 2008). The experiments below describe the *vu56* oligodendrocyte phenotype and identify *fbxw7* as the gene disrupted.

Results

Identification and characterization of the vu56 mutant phenotype

Using the *Tg(olig2:EGFP)* reporter line to assay for changes in the number and distribution of oligodendrocytes, we identified one mutation, *vu56*, which resulted in an excess of $EGFP^+$ dorsal spinal cord cells when homozygous at 3 days post fertilization (dpf) (Figure 4A, B). Whereas mutant larvae were morphologically indistinguishable from wild-type siblings (Figure 4C & D), they died by 9 dpf due to a failure to inflate swim bladders, which are required for buoyancy and feeding. Immunohistochemistry of transverse sections labeled with Sox10 antibody demonstrated that all excess dorsal $EGFP^+$ were also $Sox10^+$ as were ventral cells in positions normally occupied by OPCs (Figure 4E-H). Quantification revealed mutant larvae had approximately 1.5 fold more $Sox10^+$

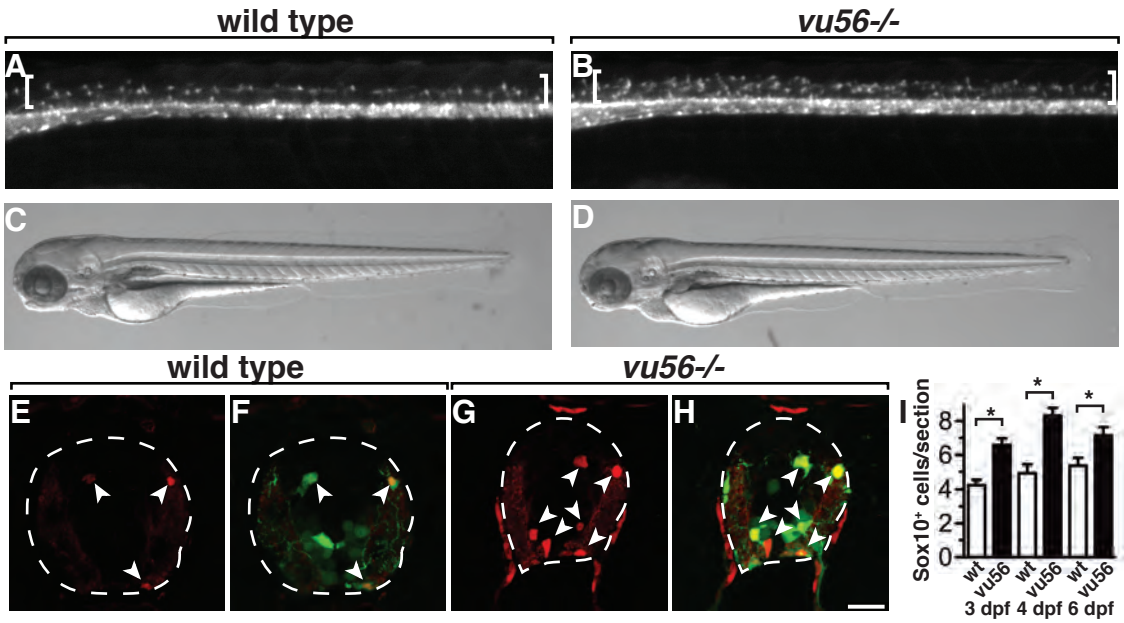

Figure 4 Identification of *vu56.* **(A-B)** Lateral views of wild-type sibling and *vu56* mutant larvae carrying the *Tg(olig2:EGFP)* reporter (dorsal OPCs marked by brackets) at 3 dpf. **(C-D)** Brightfield images of larvae from A-B. **(E-H)** Transverse sections of 3 dpf wild-type sibling and *vu56* mutants labeled with anti-Sox10 (red, arrowheads). Panels **F** and **H** are a merge with *olig2:EGFP* (green). **I** Quantification of Sox10^{+} cells per spinal cord section in wild-type sibling (wt) and *vu56* mutants at 3, 4 and 6 dpf (n=17 wild-type and 19 mutant at 3 dpf ($p<0.0001$), 7 wild-type and 10 mutant at 4 dpf ($p=0.0002$), 5 wild-type and 5 mutant at 6 dpf ($p=0.0357$)). Error bars represent SEM.

cells per section compared to wild-type siblings, which persisted through at least 6 dpf (Figure 4I).

We next investigated the extent of differentiation of the excess OPCs by expression of markers of later stages of development using in situ RNA hybridization. The myelin genes *plp1a* and *mbp* were expressed along the pial surface of the spinal cord in both wild-type sibling and *vu56-/-* larvae. However, *vu56* mutant larvae also ectopically expressed *plp1a* medially (Figure 5A-H). We also performed immunohistochemistry to detect MBP protein expression in the spinal cord. In both wild-type sibling and *vu56*-/- larvae, the myelination of the ventral longitudinal fascicles appears similar (Figure 5 I-L).

Mapping of the vu56 mutation

In order to uncover the underlying cause of the excess OPCs, it was necessary to determine the gene disrupted in *vu56* mutant larvae. To determine the mutant loci, we used a feature of DNA termed simple sequence length polymorphisms (SSLPs). SSLPs are di- or tri-nucleotide sequences repeated a variable number of times. Similar to the different strains of mice used for experiments, zebrafish also have different laboratory strains that contain different SSLP repeat lengths. We crossed heterozygous carriers with a different background strain to generate a family with recombined SSLPs. As one gets near the mutation site, SSLPs from the original mutated strain will segregate together with no recombination. Genomic DNA isolated from identified *vu56* mutants and

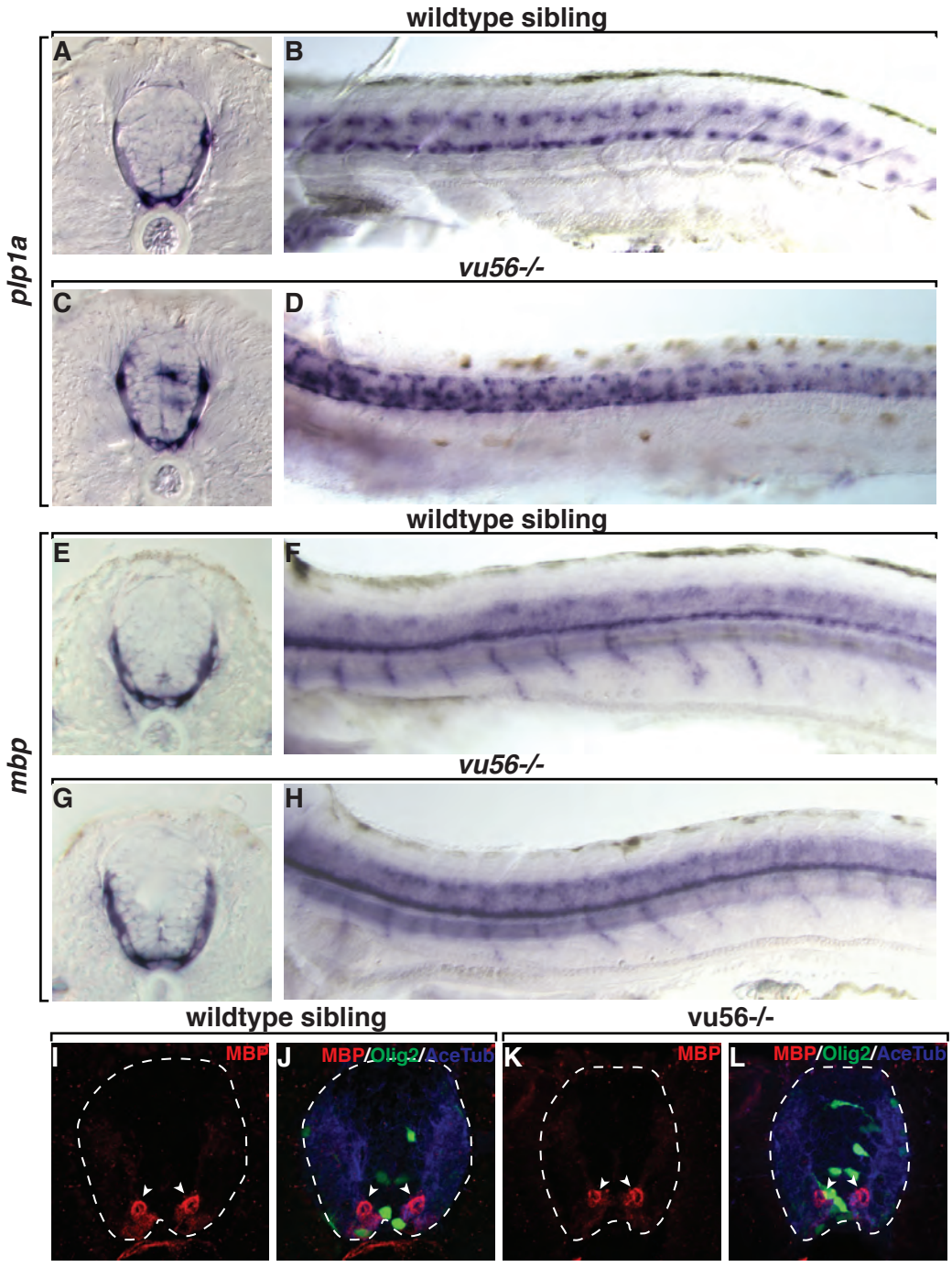

Figure 5 Excess OPCs express markers of differentiation. (A-H) Transverse **(A, C, E, G)** and lateral **(B, D, F, H)** views of wild-type sibling and *vu56* mutant larvae at 4 dpf detecting *plp1a* **(A-D)** and *mbp* **(E-H)** mRNA. **(I-L)** Transverse sections of wild-type sibling and *vu56* mutant larvae at 6 dpf labeled with anti-MBP (red, arrowheads). Panels **J, L** are merge with *olig2:EGFP* (green) and anti-acetylated tubulin (blue).

wild-type clutchmates was assayed by bulked segregant analysis (BSA) to identify a chromosomal region for the mutation. Briefly, DNA from 24 larvae each of *vu56* mutants and wild-type siblings was pooled and assayed for SSLPs that displayed different SSLP banding patterns. Characterized SSLPs in zebrafish are referred to as zmarkers and their chromosomal locations are known (Shimoda et al., 1999; Geisler et al., 2007). BSA revealed the mutation resided within a 0.6 cM region of chromosome 1. We refined the map with individual *vu56* mutant larvae to determine recombination frequencies for other SSLPs in the region.

The mutation is flanked by zmarker z63947 with 73 recombinants from a total of 454 mutant larvae for a recombination frequency of 16.1% and by zmarker z10315 with 4 recombinants from a total of 479 mutant larvae for a recombination frequency of 0.84% (Figure 6A). Within this region we identified *fbxw7* as a candidate gene because expression of human *FBXW7* was suppressed in gliomas (Gu et al., 2007).

Characterization of the fbxw7 mutation

Initially, Fbxw7 was a hypothetical protein in zebrafish based on sequence homology. Using Ensembl as a guide, we designed primers to amplify cDNA from *vu56* mutant larvae and wild-type siblings. However, we were unable to amplify full-length cDNA to look for mutations. We decided to amplify individual exons from genomic DNA because *fbxw7* contained just 12 exons. Sequencing of PCR products revealed a point mutation in what was then exon 9 that contains part of

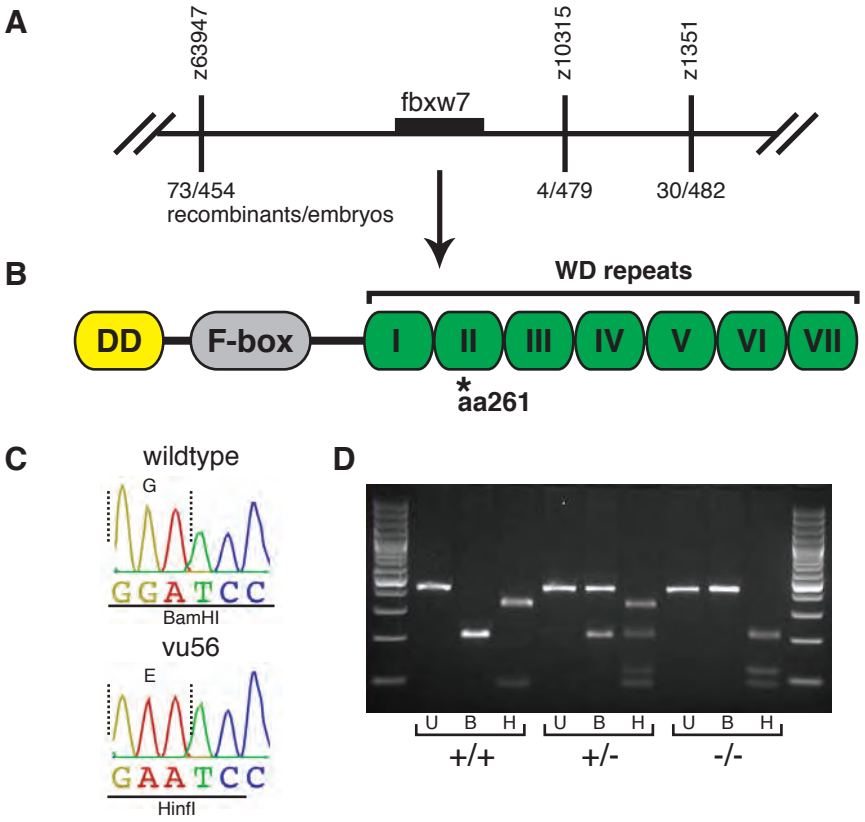

Figure 6 *vu56* maps to Chromosome 1. (A) Schematic representation of region of chromosome 1 linked to *vu56* mutation which contains *fbxw7*. **(B)** Schematic representation of Fbxw7 depicting major domains. Asterick indicates location of the amino acid substitution resulting from *vu56* mutation within the second WD repeat. **(C)** Sequence traces of wildtype and *vu56* DNA. A G-to-A transversion converted a BamHI site to a HinfI site. **(D)** RFLP genotyping of homozygous wildtype (+/+), heterozygous (+/-) and mutant (-/-) larvae. U=uncut, B=BamHI digest, and H=HinfI digest.

the second (of eight total) WD repeats. Subsequent refinement of the zebrafish genome now places the mutation within exon 8 and a total of 11 exons for *fbxw7*. The *vu56* mutation resulted in a G-to-A transversion (Figure 6C) and converts the neutral amino acid glycine to the negatively charged amino acid aspartate at the amino acid 261 position (Figure 6B). Both PolyPhen (Ramensky et al., 2002) and SIFT (Ng and Henikoff, 2001) characterize the mutation as detrimental.

Another effect of the mutation is the conversion of a Restriction Fragment Length Polymorphism (RFLP) from a BamHI site to a HinfI site. We used this RFLP to test for linkage to the *vu56* mutation. Larvae from intercrosses of heterozygous adults were assayed for the excess OPC phenotype and genotyped for the RFLP. Phenotypically identified wild-type larvae were either homozygous for the BamHI allele or heterozygous for both alleles. All 70 larvae identified as *vu56* mutants were homozygous for the HinfI allele (Figure 6D).

Validation of fbxw7 as the mutated gene producing the vu56 phenotype

Antisense morpholino oligonucleotides either inhibit translation of mRNA by binding to the translation start site or block splicing of pre-mRNA by binding to an intron-exon boundary. Splice-blocking morpholinos typically splice out the targeted exon and yield a mRNA which is shorter than wildtype, however, it is also possible to produce a larger mRNA due to intronic inclusion. We designed a morpholino with sequence recognition to the intron 3/exon 4 boundary (*fbxw7*^{SSMO}) to block splicing of the mRNA. Embryos were injected with a range

of *fbxw7*^{SSMO} doses between 2ng – 8.5ng at the one- to two-cell stage. RT-PCR amplification of RNA collected at 24 hpf displayed a higher molecular weight band indicating intronic inclusion (Figure 7A). Sequencing of the product confirmed inclusion of a portion of intron 3 that resulted in a frameshift and premature stop codon thus rendering a null protein (Figure 7B).

The lowest dose, 2 ng, phenocopied the morphology and excess dorsal GFP^{+} spinal cord cell phenotype of *fbxw7*^{vu56} (Figure 8A-D). Quantification of transverse sections labeled with Sox10 antibody demonstrated *fbxw7*^{SSMO} injected embryos display a similar excess of OPCs (Figure 8E-I). Together with the sequence and expression data, we conclude *vu56* is the result of mutation of *fbxw7* and named the allele *fbxw7*^{vu56}.

Additional experiments

We also had a translation blocking morpholino and second splice blocking morpholino designed. The translation blocking morpholino was based on the EST sequence and therefore only blocked the β-*fbxw7* isoform, although this was unknown at the time. At a 2ng dose there was no apparent morphological or EGFP phenotype (Figure 9A-D). However, at 4 ng embryos were shorter and displayed smaller heads and heart edema (Figure 9E, F). Additionally, there was a dramatic decrease in EGFP^{+} cells. We did not investigate this phenotype further as we were unsure at that point if there were multiple isoforms and if the

A

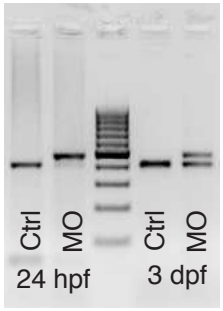

B

```
Ctrl  AGAATGGCTTCGCACCTTTCAGAGCTGGAGTGGCCCAGAGAAGCTGCTTGCACTGGATGAGTTAATCGACAGCTGTGAGCCCACACAGGTCA
MO    AGAATGGCTTCGCACCTTTCAGAGCTGGAGTGGCCCAGAGAAGCTGCTTGCACTGGATGAGTTAATCGACAGCTGTGAGCCCACACAGGTCA

Ctrl  AACATATGATGCAGGTGATCGAACCGCAGTTTCAGAGAGACTTCATCTCACTGCTACCGAGAG----------
MO    AACATATGATGCAGGTGATCGAACCGCAGTTTCAGAGAGACTTCATCTCACTGCTACCGAGAGAGCCTCACCCTCTCCTGATGTTCCTGATG

Ctrl  ----------AGTTGGCTTTGCACGTGTTGTCATTTCTGGAGCCAAAGGATCTGCTTCAGGCAGCCCAGACGT
MO    TCGGACTCTTTCTGTCTCTGTCTTGTTGTAGTTGGCTTTGCACGTGTTGTCATTTCTGGAGCCAAAGGATCTGCTTCAGGCAGCCCAGACGT

Ctrl  GTCGTTACTGGCGTATTCTAGCAGAGGACAACCTGCTCTGGAAGGAAAAATGCAAAGAAGAAGGTATTGATGAGCCCTTGCACATAAAGAGA
MO    GTCGTTACTGGCGTATTCTAGCAGAGGACAACCTGCTCTGGAAGGAAAAATGCAAAGAAGAAGGTATTGATGAGCCCTTGCACATAAAGAGA

Ctrl  AGGAAGGTCATCAAGCCGGGGTTCACACACAGTCCTTGGAAGAGTGCCTACATCAGACAACACAGAATAGACACCAACTGGAGGAGAGGA
MO    AGGAAGGTCATCAAGCCGGGGTTCACACACAGTCCTTGGAAGAGTGCCTACATCAGACAACACAGAATAGACACCAACTGGAGGAGAGGA
```

Figure 7 Effectiveness and sequencing of *fbxw7*^{SSMO}. (A) RT-PCR analysis of *fbxw7* splice blocking morpholino and uninjected control (Ctrl) and *fbxw7*^{SSMO}-injected (SSMO) 24hpf embryos and 3 dpf larvae. Upper bands in SSMO lanes (astericks) indicate splice-blocking. **(B)** Sequence alignment of RT-PCR products from control embryos and *fbxw7*^{SSMO}-injected embryos showing inclusion of intron 4. Underlined sequence indicates sequence complimentary to the splice-blocking morpholino.

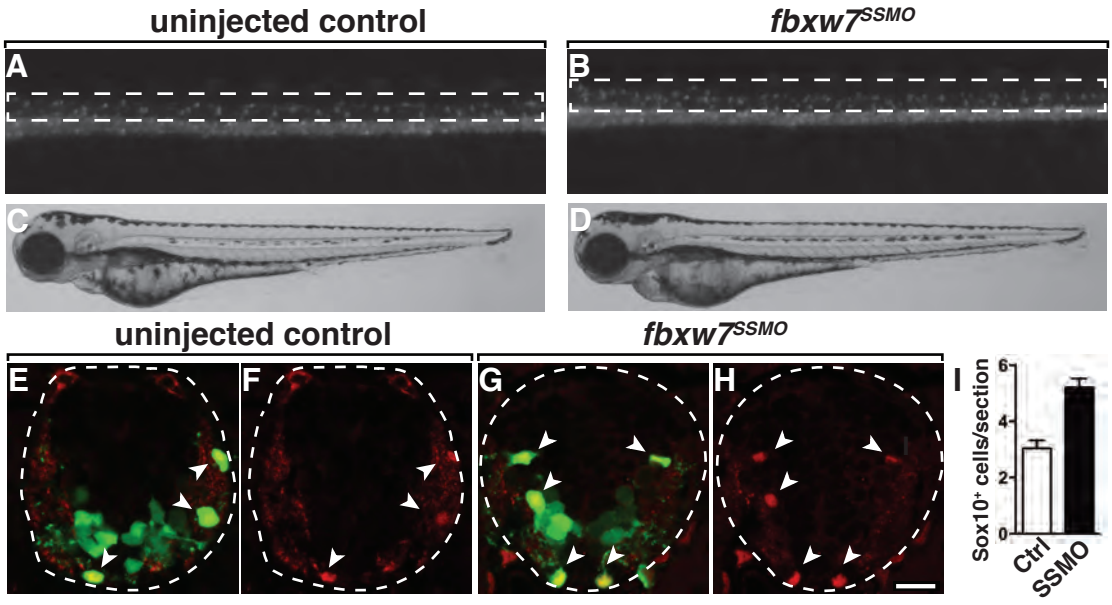

Figure 8 *fbxw7*^{SSMO} phenocopies *vu56*. (A-B) Lateral images of 3 dpf uninjected and *fbxw7*^{SSMO}-injected *Tg(olig2:EGFP)* larvae. **(C,D)** Coore-sponding brightfield images of A,B. **(E-H)** Transverse sections of 3 dpf uninjected and *fbxw7*^{SSMO}-injected *Tg(olig2:EGFP)* larvae labeled with anti-Sox10 (red, arrowheads). **(I)** Quantification of Sox10^{+} cells per section of *fbxw7*^{SSMO}-injected (n=8 per group, p=0.0001). Error bars represent SEM.

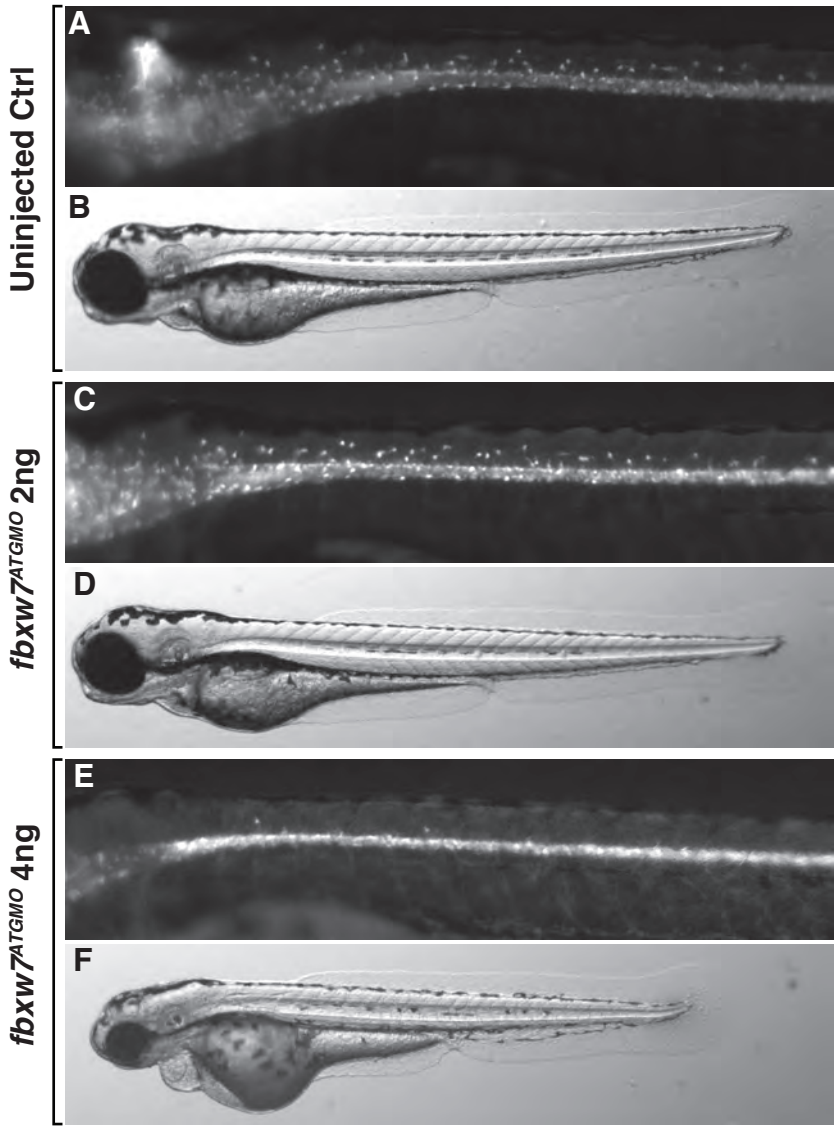

Figure 9 Translation blocking morpholino has a more severe phenotype. (A,C,E) Lateral images of 3 dpf uninjected and *fbxw7*^{ATGMO}-injected *Tg(olig2:EGFP)* larvae. **(B,D,F)** Cooresponding brightfield images of A,C,E.

result was due directly to the morpholino or off-target effects that sometimes produce cell death (ref).

The second splice blocking morpholino was designed to the splice acceptor site of exon 5 just after the F-box domain. While this morpholino did result in inclusion of a 169 bp intron and a premature stop codon (Figure 10B), the splice blocking was incomplete and the embryos displayed no apparent change in OPC number or morphological phenotype (Figure 10A and data not shown). One possible reason for the lack of efficacy could relate to the size of the intron between exons 5 and 6, which is only 169bp. The secondary structure of the RNA could be such that access to the morpholino site it blocked.

We also sought to rescue the *fbxw7*$^{vu56-/-}$ phenotype by using both mRNA and transient DNA injections. Because we were unable to clone full-length fragments from cDNA, we amplified the unique exon for each isoform and cloned it to the merged common region from the available ESTs. We constructed both myc-tagged and fusion proteins with fluorescent reporters. However, we were unable to reliably express Fbxw7. We did not attempt to rescue using *fbxw7* from another animal.

Discussion

A complete understanding of lineage progression of oligodendrocytes is important to determining what processes fail in disease and

A

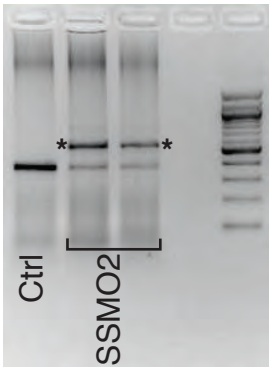

B

```
Ctrl    GAGAGTTGGCTTTGCACGTGTTGTCATTTCTGGAGCCAAAGGATCTGCTTCAGGCAGCCCAGACGTGTCGTTACTGGCGTA
SSMO2   GAGAGTTGGCTTTGCACGTGTTGTCATTTCTGGAGCCAAAGGATCTGCTTCAGGCAGCCCAGACGTGTCGTTACTGGCGTA

Ctrl    TTCTAGCAGAGGACAACCTGCTCTGGAAGGAAAAATGCAAAGAAGAAG----------------------------------
SSMO2   TTCTAGCAGAGGACAACCTGCTCTGGAAGGAAAAATGCAAAGAAGAAGGTAATATATATTTTCTTTACCTCCCCCATAAAC

Ctrl    ----------------------------------------------------------------------------------
SSMO2   TCTTTGACTTTTAAAATGTATCCCTTAACTGCATCCCAAGTATACTAAATAGTTCCCTGACTGATTTCTAGTCGGCCAAGT

Ctrl    ----------------------------------------------------GTATTGATGAGCCCTTGCACATAAAG
SSMO2   GGTATTGTGCATTGAATCATTAGTGTCACCAACATAAACCCCAACTCTATTGCAGGTATTGATGAGCCCTTGCACATAAAG

Ctrl    AGAAGGAAGGTCATCAAGCCGGGGTTCACACACAGTCCTTGGAAGAGTGCCTACATCAGACAACACAGAATAGACACCAAC
SSMO2   AGAAGGAAGGTCATCAAGCCGGGGTTCACACACAGTCCTTGGAAGAGTGCCTACATCAGACAACACAGAATAGACACCAAC

Ctrl    TGGAGGAGAGGGGACCTCAAGTCACCTAAGGTGTTGAAAGGCCATGACGACCATGTCATCACCTGCCTCCAGTTCTGTGGA
SSMO2   TGGAGGAGAGGAGACCTCAAGTCACCTAAGGTGTTGAAAGGCCATGACGACCATGTCATCACCTGCCTCCAGTTCTGTGGA

Ctrl    AACCGCATAGTGAGCGGCTCAGACGACAACACGCTCAAAGTGTGGTCTGCTGTTACTGGGAA
SSMO2   AACCGCATAGTGAGCGGCTCAGACGACAACACGCTCAAAGTGTGGTCTGCTGTTACTGGGAA
```

Figure 10 Effectiveness and sequencing of *fbxw7*^{SSMO2}. (A) RT-PCR analysis of second *fbxw7* splice blocking morpholino and uninjected control (Ctrl) and *fbxw7*^{SSMO2}-injected (SSMO2) 24hpf embryos. Upper bands in SSMO2 lanes (astericks) indicate splice-blocking. **(B)** Sequence alignment of RT-PCR products from control embryos and *fbxw7*^{SSMO2}-injected embryos showing inclusion of intron 5. Underlined sequence indicates sequence complimentary to the splice-blocking morpholino.

how to activate an appropriate response to repair damage. Many signaling pathways are known to play roles during oligodendrocyte development. Shh is critical for specification of precursors in the ventral domain of the spinal cord (Orentas et al., 1999). Notch signaling has been demonstrated to inhibit neurogenesis to maintain a population of precursors for subsequent production of oligodendrocytes (Wang et al., 1998; Park and Appel, 2003). Additionally several growth factors are known to induce proliferation of OPCs, including PDGF-AA, fibroblast growth factor 2 (FGF2), and insulin growth factor 1 (IGF-1) (Barres and Raff, 1994; McMorris and McKinnon, 1996; Baron et al., 2002). Some of the pathways activated by these factors are also important during oligodendrocyte differentiation. PI3K (phosphoinositol 3-kinase) has been shown to be an intracellular mediator of PDGF signaling (Ebner et al., 2000). The integration of the known factors and signaling pathways to drive differentiation forward by inducing cell cycle exit and production of myelin is not well understood.

During a forward genetic screen in zebrafish to uncover novel mechanisms regarding oligodendrocyte development, we identified a mutation *vu56*, which produced an excess number of OPCs. Mapping and sequencing of the mutation revealed a missense mutation in *fbxw7*. Fbxw7 is an E3 ubiquitin ligase important for the degradation of several proteins involved in cell cycle progression, including c-myc, Cyclin E, and Notch (Welcker and Clurman, 2008). Indeed, many cancers are known to have mutations in targets of Fbxw7 that render them insensitive to regulation by Fbxw7 (Bahram et al., 2000; Gregory

and Hann, 2000; Weng et al., 2004) or in Fbxw7 itself (Kemp et al., 2005; Lee et al., 2006; Akhoondi et al., 2007; O'Neil et al., 2007; Thompson et al., 2007). Fbxw7 expression may also be deregulated in cancer as evidenced by a repression of *fbxw7β* in gliomas, a cancer of the CNS (Gu et al., 2007). Also, *fbxw7* heterozygous mice in combination with p53 heterozygousity have an increased incidence of tumors following radiation, indicating *fbxw7* is a haploinsufficient tumor suppressor (Mao et al., 2004).

A curiosity with the *fbxw7*$^{vu56-/-}$ phenotype is the relatively normal morphology of the embryos. This can be accounted for by the nature of the mutation, a missense allele. Fbxw7 function may therefore only be partially decreased by the mutation. In agreement with this reasoning, increasing doses of *fbxw7*^{SSMO} resulted in more severe morphological phenotypes, which is also consistent with the reported mouse knockout that dies embryonically around E9.5 (Tetzlaff et al., 2004; Tsunematsu, 2004).

One now must ask how does Fbxw7 fit into the development of the oligodendrocyte lineage? Fbxw7 is known to regulate several cell cycle regulators. FGF2, alone and in combination with IGF-I, has been demonstrated to enhance cdk2 activity and association with Cyclin E, a protein regulated by Fbxw7 (Frederick and Wood, 2004). Additionally, previous results from the lab demonstrated another target of Fbxw7, Notch, is required during oligodendrocyte specification (Park and Appel, 2003). One or both of these proteins could be contributing to the excess OPCs in *fbxw7*$^{vu56-/-}$ larvae.

CHAPTER IV

EXCESS OPCS ARISE FROM VENTRAL SPINAL CORD PRECURSORS

The cloning of individual isoform exons was performed with the help of Macie Walker, post-doctoral researcher. RNA in situ hybridizations for the isoforms, BrdU and Sox2 immunohistochemistry were performed with the help of Christina Kearns, lab manager.

Introduction

During development, cells of the central nervous system (CNS) must be produced at precise times and positions. Uncovering the mechanisms that generate the various neuronal and glial cell types is important to understanding both the normal architecture and functions of the CNS, as well as the defects caused by disease and injury. In particular the mechanisms that drive differentiation of oligodendrocytes from precursor to mature oligodendrocyte with compact myelin are not well understood.

Opposing morphogen gradients in the spinal cord produce expression patterns of several transcription factors required for the specification of various cell types. Ventrally, sonic hedgehog (Shh) is initially expressed by the notochord to induce the floor plate which then also expresses Shh. Diffusion of Shh dorsally results in a graded induction of the Shh signaling pathway and expression of transcription factors within distinct precursor domains (Ericson et al., 1996; Tanabe and Jessell, 1996; Briscoe et al., 2000). Each domain then gives rise to a

particular set of neurons and glia. Dorsally, bone morphogenetic protein (BMP) is expressed in the roof plate and diffuses ventrally to induce the dorsal precursor domains of neurons and glia (Tanabe and Jessell, 1996).

Oligodendrocytes arise from a ventral precursor domain termed pMN, precursor of Motor Neuron, which also produces motor neurons. Disruption of the morphogen Shh results in a ventral expansion of dorsal markers and loss of ventral cells types, including oligodendrocytes (Chiang et al., 1996; Ericson et al., 1996). Deletion of transcription factors also affects specification within the spinal cord. Loss of *olig2* results in loss of all pMN domain cell types and expansion of the p2 domain V2 interneurons (Lu et al., 2002; Takebayashi et al., 2002; Zhou and Anderson, 2002).

Positional cloning revealed a missense mutation in *fbxw7* in *vu56* mutants. Fbxw7 is the substrate recognition component of the SCF ubiquitin ligase complex (Welcker and Clurman, 2008). Poly-ubiquitination leads to protein degradation by the proteasome. We demonstrate *fbxw7* is expressed in the spinal cord during OPC specification. We also determine that zebrafish, like other vertebrates, express 3 isoforms of *fbxw7* (α, β, and γ) that are differentially expressed throughout the embryo.

Several questions arise concerning the relationship between *fbxw7* and OPC specification. Is *fbxw7* expressed within OPCs or precursor cells? Which cells generate the excess OPCs? We investigated the expression profiles of each isoform of *fbxw7* at critical timepoints of oligodendrocyte development. Excess

OPCs could be from a cell fate error due to a failure of motor neuron specficiation, a general overgrowth of the spinal cord, or increased division of precursors or OPCS. We determined *fbxw7-α* and *fbxw7-β* are expressed at the right time and place during OPC specification. We also provided evidence that the excess OPCs arise from neural precursors in the pMN domain.

Results

Expression of fbxw7 during development

We investigated the *fbxw7* temporal and spatial expression to determine if it is consistent with the *fbxw7*^{vu56} phenotype. We first identified an expressed sequence tag (EST), EB835996, which contained the N-terminal half of *fbxw7*. A second EST, EG571371, contained the C-terminal sequence, a poly-A tail, and overlapped with EB835997. Splicing the two ESTs together produced a full-length cDNA that contained a transcriptional start site and a polyA tail. We used this spliced construct to design a RNA in situ hybridization probe that would detect all *fbxw7* transcripts. Wild-type embryos from bud-stage (~10 hpf) through 3 dpf were assayed for expression of EB835996. At bud-stage, *fbxw7* was expressed in the neuroectoderm from which the central nervous system develops (Figure 11 A & B). By 24 hpf, expression is ubiquitous, though a distinct striped pattern is observed in the hindbrain that is reminiscent of rhombomeric boundaries (Figure 11 C & D). Later at 36 hpf when OPCs begin to be specified, expression has

decreased in the muscle, but is still prominent in the brain and spinal cord as well as along the pronephric ducts and fin folds (Figure 11 E & F).

Identification of zebrafish fbxw7 isoforms

Mammals possess three isoforms of Fbxw7, α, β, and γ, which are transcribed from unique 5' exons and joined to a common set of 10 exons (reviewed in (Welcker and Clurman, 2008)). Two of the unique exons contain dominant localization signals: α exon has a basic nuclear localization sequence (NLS) and β has a hydrophobic transmembrane domain (Welcker et al., 2004). However, γ does not contain any signal and localizes to the nucleolus due to a signal in the common region (Welcker et al., 2004). The question then arises if zebrafish also contain multiple isoforms of *fbxw7*.

We determined the EST used for probe synthesis, EB835996, contained sequence with homology to the β isoform (Figure 12 A). As with *Xenopus* β-*fbxw7* (Almeida et al., 2010), the zebrafish β-*fbxw7* exon is shorter than the mammalian homolog and does not possess the hydrophobic domain (Figure 12 A).

In order to detect other isoforms, we used 5'RACE technology to identify the 5' end of *fbxw7*. cDNA generated from RNA isolated from 24 hpf embryos was used as the input for the Roche 5'/3' RACE kit. A fragment of approximately 440bp was amplified. Sequencing of the product revealed homology to the mammalian γ exon. We designated this isoform as γ-*fbxw7*. However, two

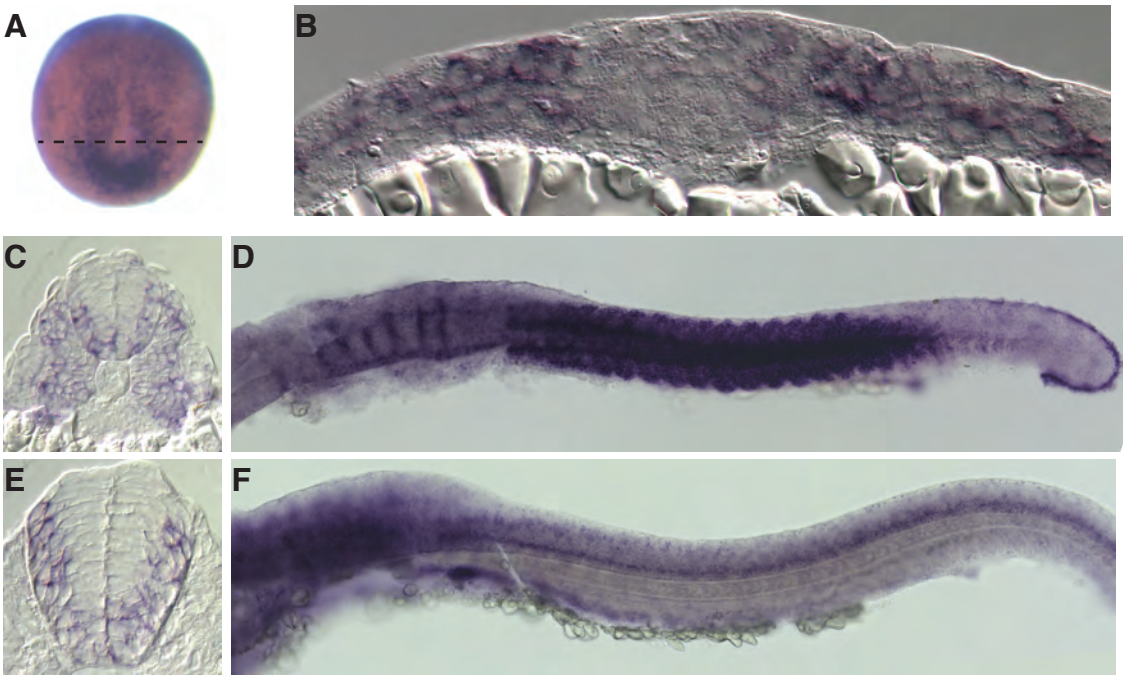

Figure 11 Pan-expression of *fbxw7* during development. (A) Ventral view of whole-mount neural plate stage embryo. **(B)** Transverse section of dashed line in (A). **(C-D)** Expression at 24 hpf. **(E-F)** Expression at 36 hpf.

interesting points can be made here 1) we were only able to amplify product related to the γ isoform not β that we knew zebrafish expressed because of the EST data and 2) we also did not amplify any sequence corresponding to an α exon. One possibility for the lack of β-*fbxw7* could be due to a low abundance at the timepoint we collected RNA. A second possibility could be the stability of both β-*fbxw7* and α-*fbxw7* isoforms.

Identification of the α isoform was more difficult, as we were initially unable to amplify full-length cDNA based on sequence from Ensembl! that was predicted to have homology to mammalian α-*fbxw7*. We turned to ESTs to identify one that might contain the α isoform. BM829297 had published sequence similar to the mammalian α exon. However, with an EST it is common for only a portion of the inserted fragment to be sequenced, meaning that the EST clone could contain a significant portion, or even the full-length, of a gene. Upon sequencing in our hands, BM829297 did contain sequence corresponding to the α exon, however, at just where the exon should splice to the first exon of the common region the sequence no longer aligns to *fbxw7*. BLAT analysis of the remaining sequence places it on a different chromosome, likely indicating an error during the production of the EST. However, armed with this α exon sequence, and the C-terminus from β, we designed primers to amplify full-length α-*fbxw7* cDNA.

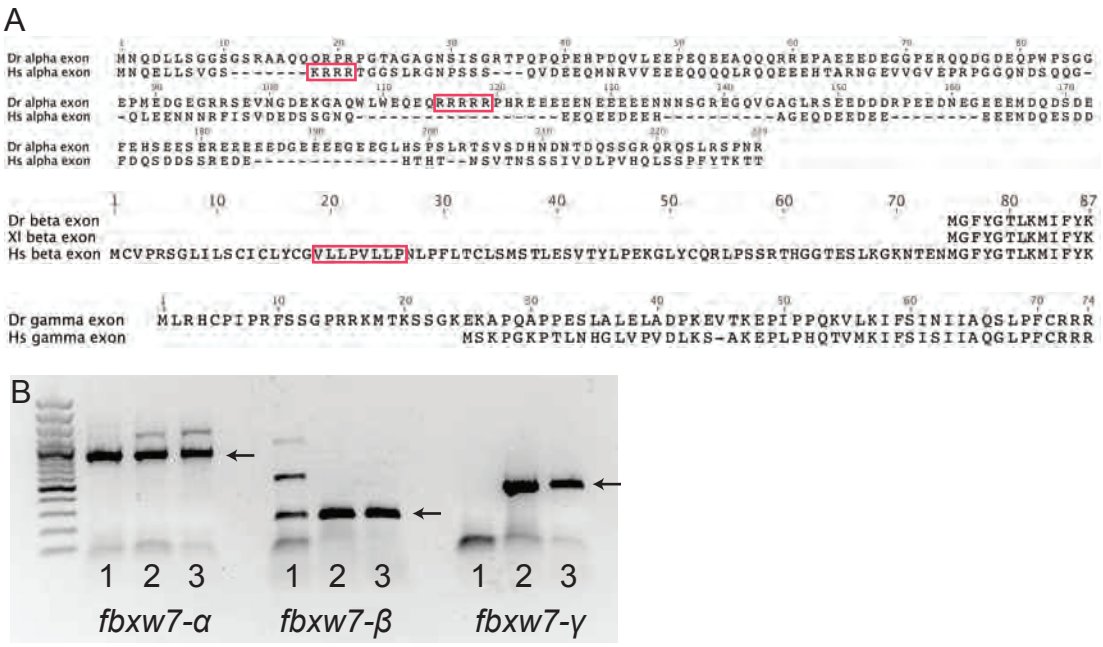

Figure 12 Zebrafish *fbxw7* isoforms. (A) Alignment of each isoform specific exon. Dr = *Danio rerio*, Hs = *Homo sapiens*, Xl = *Xenopus laevis*. Boxes in alpha indicate nuclear localization signals. Box in beta indicates hydrophobic domain. **(B)** RT-PCR Expression of each isoform during zebafish development. 1 = one-cell stage embryos, 2 = 24 hpf, and 3 = 48 hpf. Arrows indicate correct band for each isoform.

Expression of fbxw7 isoforms during development

We next looked at the expression of each isoform during development using both RT-PCR and RNA *in situ* hybridization. RT-PCR of RNA harvested from one-cell stage embryos produced α and β products, but not γ, whereas 24 hpf, and 3 dpf embryos produced all three isoforms (Figure 12 B). These results demonstrate α-*fbxw7* and β-*fbxw7* are maternally deposited, whereas all three isoforms are transcribed during later stages of development.

RNA probes for each isoform were produced using fragments amplified from genomic DNA that included some 5' UTR in order to generate probes of sufficient size to recognize each isoform. We performed RNA *in situ* hybridization at 24, 30 and 36 hpf, corresponding to the approximate times when neurogenesis ceases and just when oligodendrogenesis begins, respectively. Both α and β isoforms displayed ubiquitous expression and diffuse spinal cord expression at 24 hpf (Figure 13 A & B). By 30 hpf however, expression of both isoforms in the spinal cord was restricted to the medial septum and outer lateral edges (Figure 13 D & E). At 36 hpf, *fbxw7*-α continues to be expressed at high levels along the medial septum while *fbxw7*-β expression was weaker and restricted to the ventral spinal cord (Figure 13 G & H). *fbxw7*-γ was expressed in the somites and not expressed the spinal cord at any timepoint (Figure 13 C, F, & I).

Motor neuron number unchanged in fbxw7^{vu56} mutants

To investigate the source of the excess OPCs, we investigated several possibilities. One mechanism for the excess OPCs is a fate switch error such that cells normally fated to give rise to motor neurons fail to do so and subsequently produce oligodendrocytes. To test this, we quantified the number of motor neurons in transverse sections using anti-Islet1/2 (anti-Isl) to label all primary and secondary motor neurons in the spinal cord (Figure 14 A & B). This antibody also labels some sensory neurons in the very dorsal aspect of the spinal cord, however these cells are easy to distinguish based on location and were not included in the counts. At 3 dpf *vu56*$^{-/-}$ embryos had no change in the number of Isl^{+} cells per section compared with wild-type siblings (Figure 14 C).

A second mechanism is disruption of the all cell types in the spinal cord of *vu56*$^{-/-}$ embryos. We used anti-Zrf-1 to look at radial glial fibers, anti-Zn-8 to look specifically at secondary motor neurons, and anti-HuC as a pan-neuronal marker. All marker expression appeared normal in *vu56*$^{-/-}$ embryos (Figure 14 D-I).

pMN precursors produce the excess OPCS in fbxw7^{vu56} mutants

A third mechanism for the excess OPCs is excessive division after specification. We tested this by time-lapse imaging. During zebrafish development, spinal cord OPCs begin to migrate from their ventral origin at approximately 48 hpf in an anterior to posterior wave. We imaged multiple embryos of one clutch produced from an intercross of *vu56*$^{+/-}$ carriers from 48

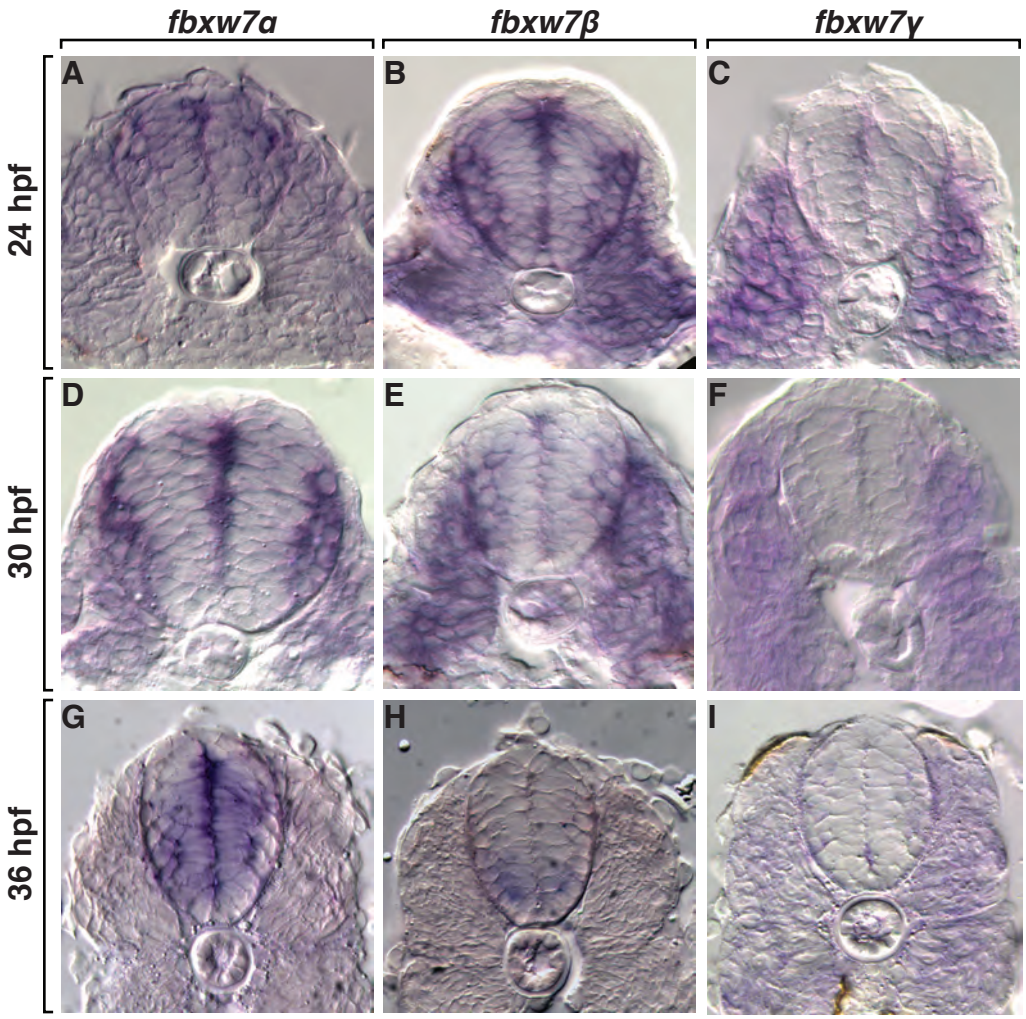

Figure 13 Expression of *fbxw7* isoforms. (A-I) Transverse sections of embryos detecting RNA expression of *α, β,* and *γ* isoforms.

hpf, when migration first begins, through 72 hpf, when most migration is complete. Embryos were genotyped after completion of the time-lapses. Over the course of the time-lapses we were able to observe division of OPCs, both in wild-type siblings and *fbxw7*$^{vu56-/-}$ embryos. We quantified the number of divisions observed for *fbxw7*$^{vu56+/+}$, *fbxw7*$^{vu56+/-}$, and *fbxw7*$^{vu56-/-}$ embryos. We did not observe more divisions on a per cell basis in *fbxw7*$^{vu56-/-}$ embryos nor did we observe any OPCs that divided more than once (Figure 15 E). However, we did notice an apparent increase in the number of cells that migrated dorsally from the ventral precursor domain (Figure 15 A – C''). Quantification of the number of OPCs occupying the dorsal from 48 hpf and 63 hpf revealed *fbxw7*$^{vu56+/+}$ embryos had an average of 17 dorsal OPCs between somites 5-9, *fbxw7*$^{vu56+/-}$ embryos had an average of 23 OPCs, and *fbxw7*$^{vu56-/-}$ embryos had an average of 40 OPCs (Figure 15 D).

In order to assess the number of precursor cells of the pMN domain, we performed immunohistochemistry to detect Sox2 expression, a marker of precursor cells in the spinal cord (reviewed in (Wegner and Stolt, 2005)). Labeling of transverse sections of 3 dpf larvae revealed an increase in the number and dorsal-ventral distribution of Sox2^{+} cells in *fbxw7*$^{vu56-/-}$ larvae (Figure 16 A-D). We also performed a 5-bromo-2'deoxyuridine (BrdU) incorporation assay at 3 dpf. *fbxw7*^{vu56} mutants had more than double the number of BrdU^{+} and BrdU^{+}/*olig2*:EGFP^{+} compared to wildtype siblings (Figure 16 E-H). These results

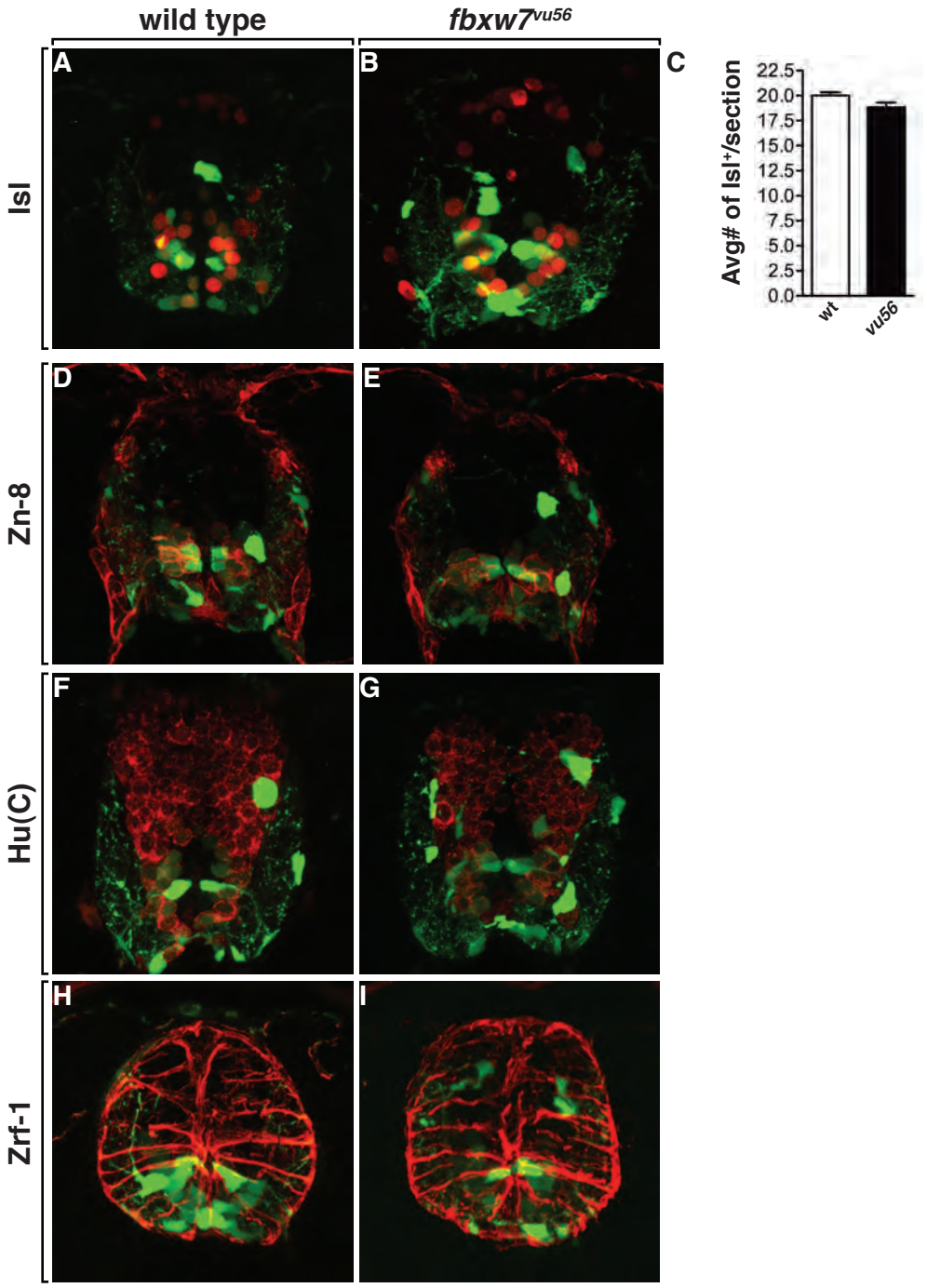

Figure 14 Spinal cord morphology is grossly normal in *fbxw7*^{vu56}. (A-B) Transverse sections of 3 dpf wild-type sibling and *fbxw7*$^{vu56-/-}$ embryos labeled with anti-Isl to marker motor neurons. **(C)** Quantification of Isl^{+} cells per section of wild-type (wt) and *fbxw7*$^{vu56-/-}$ (*vu56)* (n = 19 wild-type and 17 mutant larvae; p = 0.7658). **(D-I)** Immunohistochemistry of transverse sections of 3 dpf wild-type sibling and *fbxw7*$^{vu56-/-}$ embryos for spinal cord markers of secondary motor neurons (Zn-8), all neurons (Hu(C)), and radial glial fibers (Zrf-1).

demonstrate that *fbxw7*^{vu56} mutants maintain an increased number of dividing neural precursors that are available to generate OPCs.

Discussion

Earlier studies have shown distinct expression patterns of each *fbxw7* isoform within mouse tissues and by selective loss in cancers, such as glioblastomas. Our results follow these reports with more ubiquitous expression of α-*fbxw7*, CNS restricted expression of β-*fbxw7*, and somite expression of γ-*fbxw7*. As both α-*fbxw7* and β-*fbxw7* are expressed within the precursor domain in the CNS, Fbxw7 could be important in regulating the neural precursor population during development. Indeed, previous studies of Fbxw7 have demonstrated a role in maintaining cells in a quiescent state. Evidence for this role is demonstrated by a conditional knockout of *fbxw7* in hematopoietic lineage cells that leads to a depletion of hematopoietic stem cells (Matsuoka et al., 2008).

In mice, complete ablation of *fbxw7* results in early embryonic lethality around E10.5 due to defects in vascular, heart, and hematopoietic development (Tetzlaff et al., 2004; Tsunematsu, 2004). This early lethality has precluded studying the effect of loss of Fbxw7 during CNS development until recently. Two groups have published results using a Nestin-Cre transgenic to conditionally ablate Fbxw7 specifically in the CNS (Hoeck et al., 2010; Matsumoto et al., 2011). Both groups describe cellular defects resulting from a differentiation failure of neurons, indicating precursors are maintained. However, Hoeck et al. notes a

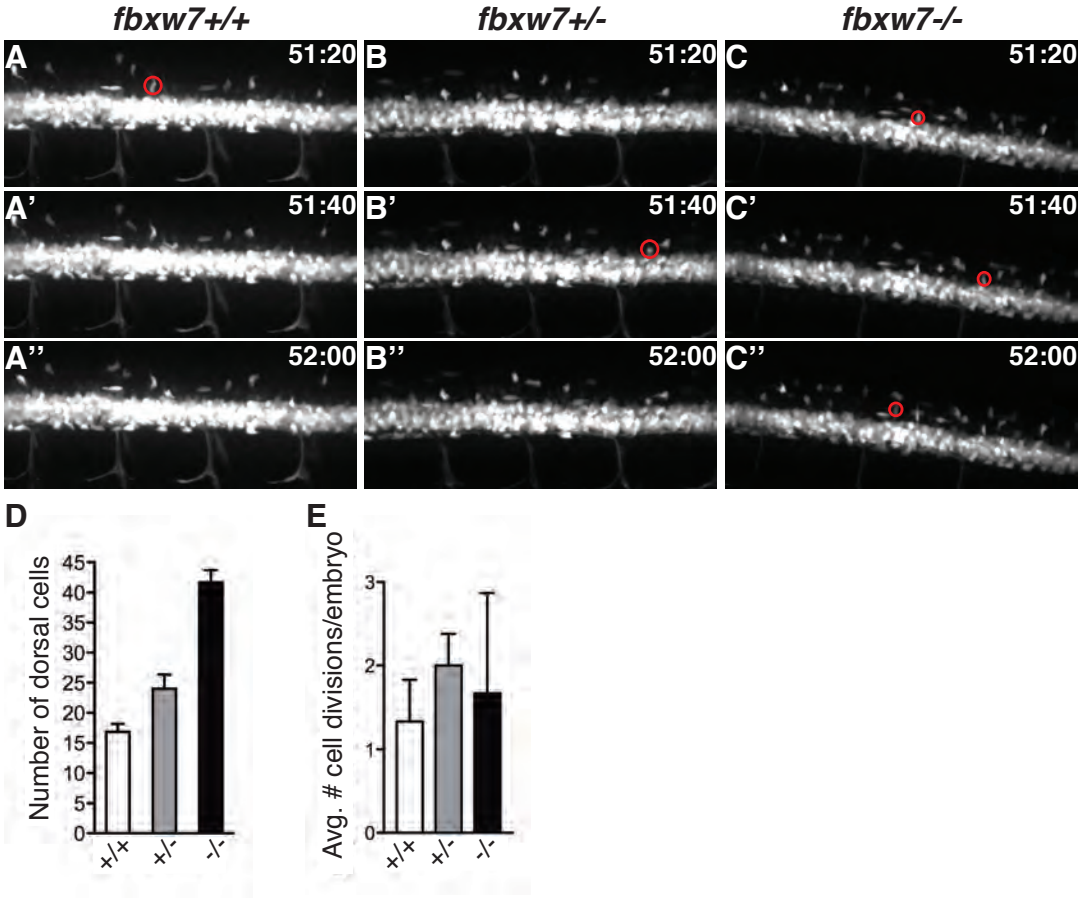

Figure 15 Timelapse imaging reveals excess OPCs in *fbxw7*$^{vu56-/-}$ arise from ventral spinal cord precursors. (A-C'') ** Lateral images of spinal cord from time-lapse movies of *Tg(olig2:EGFP)* transgenic *fbxw7*$^{+/+}$ **(A-A''), *fbxw7*$^{+/-}$ **(B-B'')**, *fbxw7*$^{-/-}$ **(C-C'')**. Numbers indicate elapsed time (hours:minutes). Red circles indicate newly migrated OPCs from the ventral domain. **(D)** Quantification of the number of cells in *fbxw7*$^{+/+}$ (n = 6), *fbxw7*$^{+/-}$ (n = 8) and *fbxw7*$^{-/-}$ (n = 3) larvae from 48 to 63 hpf. **(E)** Quantification of the average number of OPC divisions for each genotype.

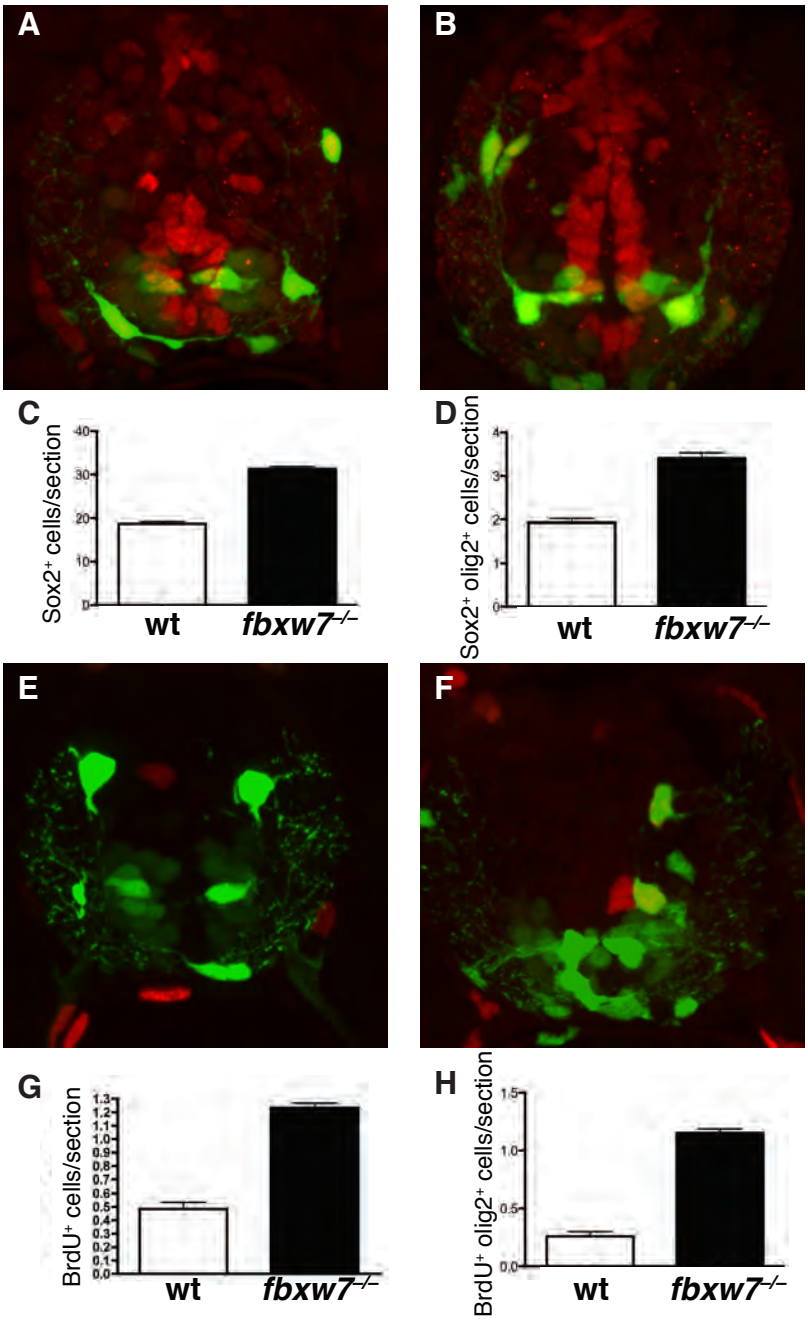

Figure 16 Increase in markers of proliferation in *fbxw7*^{vu56} mutants. (A-B) Transverse sections of wild-type and *fbxw7*^{vu56} at 3 dpf spinal cords labeled with anti-Sox2 antibody to mark neural precursors (red) in combination with *olig2*:EGFP expression. **(C-D)** Quantification of total Sox2^{+} **(C)** and Sox2^{+}/*olig2*:EGFP^{+} cells per section in wild-type and mutant larvae (n=17 wild-type and 16 mutant larvae, p<0.0001). **(E-F)** Transverse sections of wild-type and *fbxw7*^{vu56} at 3 dpf labeled to detect BrdU incorporation (red) in combination with *olig2*:EGFP expression. **(G-H)** Quantification of total BrdU^{+} and BrdU^{+}/*olig2*:EGFP^{+} cells per section in wild-type and mutant larvae (n=18 wild-type and 15 mutant larvae, p<0.0001). Error bars represent SEM.

loss of precursors due to cell death. Loss of the *Drosophila* homolog *archipelago* (*ago*) in the head and eye results in a small eye phenotype due to apoptosis that is suppressed when combined with mutations of proapoptotic genes (Nicholson et al., 2009). However, it is worth noting that the effect is constrained to the eye as other tissues in the head show an overgrowth phenotype, indicating regional differences due to *fbxw7* loss.

Additionally, neither group observed a change in oligodendrocyte number within the brain or neurosphere cultures. Matsumoto et al. did observe an increase in astrogenesis that they attributed to a cell fate switch between neurogenesis and astrogenesis. These results are in contrast to our own which show no change in motor neuron number and an increase in oligodendrocyte number. As the development of astrocytes in zebrafish has not been extensively studied, we cannot rule out an effect of *fbxw7*^{vu56} on astrogenesis in zebrafish. A common marker of astrocytes is glial fibrillary acidic protein (GFAP). GFAP is highly enriched along the fibers of radial glia cells in the spinal cord and recognized by the zrf-1 antibody. Our results demonstrate these fibers are unchanged in *fbxw7*$^{vu56-/-}$ mutants. However, as the cell bodies are not labeled, we cannot perform counts to determine astrocyte number. Recent research has investigated the role of astrocytes during regeneration of the zebrafish eye or forebrain following injury (Baumgart et al., 2012; Neve et al., 2012).

Several possibilities could account for the differences between neurogenesis and oligodendrogenesis in the different mutants. One possibility is

the presence of a second *fbxw7*-like gene in zebrafish that compensates for the loss-of-function of *fbxw7*^{vu56}. We were unable to detect a duplicate gene from our zebrafish genome queries. A second possibility is the effect of the number of OPCs at the stages observed. Cell density in vitro, growth factor availability, and cell-cell contact inhibition are known to regulate OPC number (Zhang and Miller, 1996; Calver et al., 1998; van Heyningen et al., 2001; Kirby et al., 2006). Therefore timing of analysis might produce different results. A third possibility is the mouse transgenics used result in a complete knockout of *fbxw7* within the CNS, while *fbxw7*^{vu56} is a missense mutation throughout the embryo that may not be a complete loss of function allele. Many human *FBXW7* alleles implicated in cancer are missense alleles (Akhoondi et al., 2007). Additionally, a mouse missense *Fbxw7* allele was shown to have a distinct effect that was different from a null allele during lung development (Davis et al., 2011). While our splice-blocking morpholino was designed to produce a truncated Fbxw7, its effectiveness at low doses was incomplete and phenocopied *fbxw7*^{vu56}.

Our results support a model in which Fbxw7 expression within neural precursors is required for production of normal numbers of OPCs. Many of targets of Fbxw7 are involved in cell proliferation and could account for the increased division of neural precursors. The most notable of the targets is Notch, which has been demonstrated to be involved in maintaining a precursor pool in the spinal cord.

CHAPTER V

FBXW7 REGULATION OF NOTCH DURING OLIGODENDROGENESIS

Christina Kearns, lab manager, performed quantitative PCR experiments.

Introduction

The previous chapters described the characterization and gene identification of the zebrafish mutant *fbxw7*^{vu56}. However, the mechanism by which the mutation produced the *fbxw7*$^{vu56-/-}$ phenotype was not clear. Fbxw7 negatively regulates several proteins involved in cell cycle progression, including Cyclin E, c-myc, c-Jun, and Notch (ref).

Fbxw7 was first isolated as the cell division cycle mutant Cdc4 in yeast (Hereford and Hartwell, 1974). A homologue, Sel-10, was subsequently identified in *C. elegans* as a negative regulator of Lin-12, a Notch homologue (Hubbard et al., 1997). Complete knockout of *fbxw7* in mice resulted in embryonic lethality around E10.5 of vascular defects due to misregulation of Notch (Tetzlaff et al., 2004; Tsunematsu, 2004). The role of Notch in vascular development has been well characterized (reviewed by (Gridley, 2010).

In addition to a role in vascular development, Notch signaling is also known to affect many cell fate decisions in a variety of tissues during development. Typically loss of Notch signaling results in the formation of one cell type at the expense of another. This is no different during spinal cord development. Notch is utilized several times in the developing CNS, in particular

with oligodendrogenesis. First in the pMN domain, Notch signaling promotes the maintenance of precursors during neurogenesis to allow for oligodendrocyte formation later as demonstrated by experiments that alter the Notch pathway. Loss of Notch signaling results in loss of precursor cells and formation of excess neurons at the expense of glia, such as oligodendrocytes (Chitnis et al., 1995; de la et al., 1997; Appel and Eisen, 1998; Appel et al., 2001; Itoh et al., 2003; Park and Appel, 2003; Imayoshi et al., 2010). Conversely, overexpression of the NICD results in the formation of excess oligodendrocyte lineage cells at the expense of motor neurons (Zhou et al., 2001; Park and Appel, 2003). Later during oligodendrogenesis, Notch signaling inhibits the differentiation of OPCs into mature oligodendrocytes (Wang et al., 1998; Gaiano et al., 2000; Tanigaki et al., 2001; Park and Appel, 2003). How Notch is regulated to control both maintenance of precursors and inhibition of differentiation is not well understood.

The intracellular domain of Notch is targeted for degradation by Fbxw7-mediated ubiquitination (Gupta-Rossi, 2001; Oberg, 2001; Wu et al., 2001). Therefore, elevated Notch signaling could result in excess OPC formation. We tested if aberrant Notch signaling produced the excess OPC phenotype of *fbxw7*^{vu56} mutants. Gene expression and transgenic reporter analysis demonstrate an increase in Notch activity. Further, we show that modulating Notch signaling suppresses the *fbxw7*^{vu56} mutant phenotype. Recent work with brain-specific knockout of *fbxw7* also implicates Fbxw7-regulated Notch and c-

Jun in controlling neural cell survival and differentiation, as well as formation of astrocytes (Hoeck et al., 2010; Jandke et al., 2011; Matsumoto et al., 2011).

Results

Notch activity is upregulated in fbxw7$^{vu56-/-}$ embryos

Fbxw7 negatively regulates Notch by targeting phosphorylated NICD for degradation by the proteasome (Gupta-Rossi, 2001; Wu et al., 2001). Therefore, misregulation of NICD degradation could be responsible for the excess OPCs in *fbxw7^{vu56}* larvae.

We used the transgenic Tg*(Tp1bglob:hmgb1-mCherry)* reporter line (hereafter *Tp1*:mCherry) designed with repeats of the NICD RBP-Jκ regulatory elements driving expression of mCherry to assay Notch activity. Transverse sections revealed an increase in the number of *Tp1*:mCherry^{+} cells at both 20 hpf and 3 dpf in *fbxw7$^{vu56-/-}$* mutants, particularly along the medial septum compared with wild-type siblings (Figure 17 A-H). Additionally, olig2^{+} OPC cells in *fbxw7$^{vu56-/-}$* larvae also had weak *Tp1*:mCherry expression that was not present in wild-type siblings (Figure 17 compare B to D and E to G). Whole-mount imaging at 6 dpf also showed an increase in the number of *Tp1*:mCherry^{+} cells including among *olig2*$^{+}$ cells along the ventral domain in the pMN domain (Figure 17 I &J).

To further confirm the increased Notch activity we used quantitative PCR (qPCR) to assay for downstream targets. Expression of *her4.1* RNA at 4 dpf was increased nearly 3-fold higher in *fbxw7$^{vu56-/-}$* larvae compared to wild-type larvae

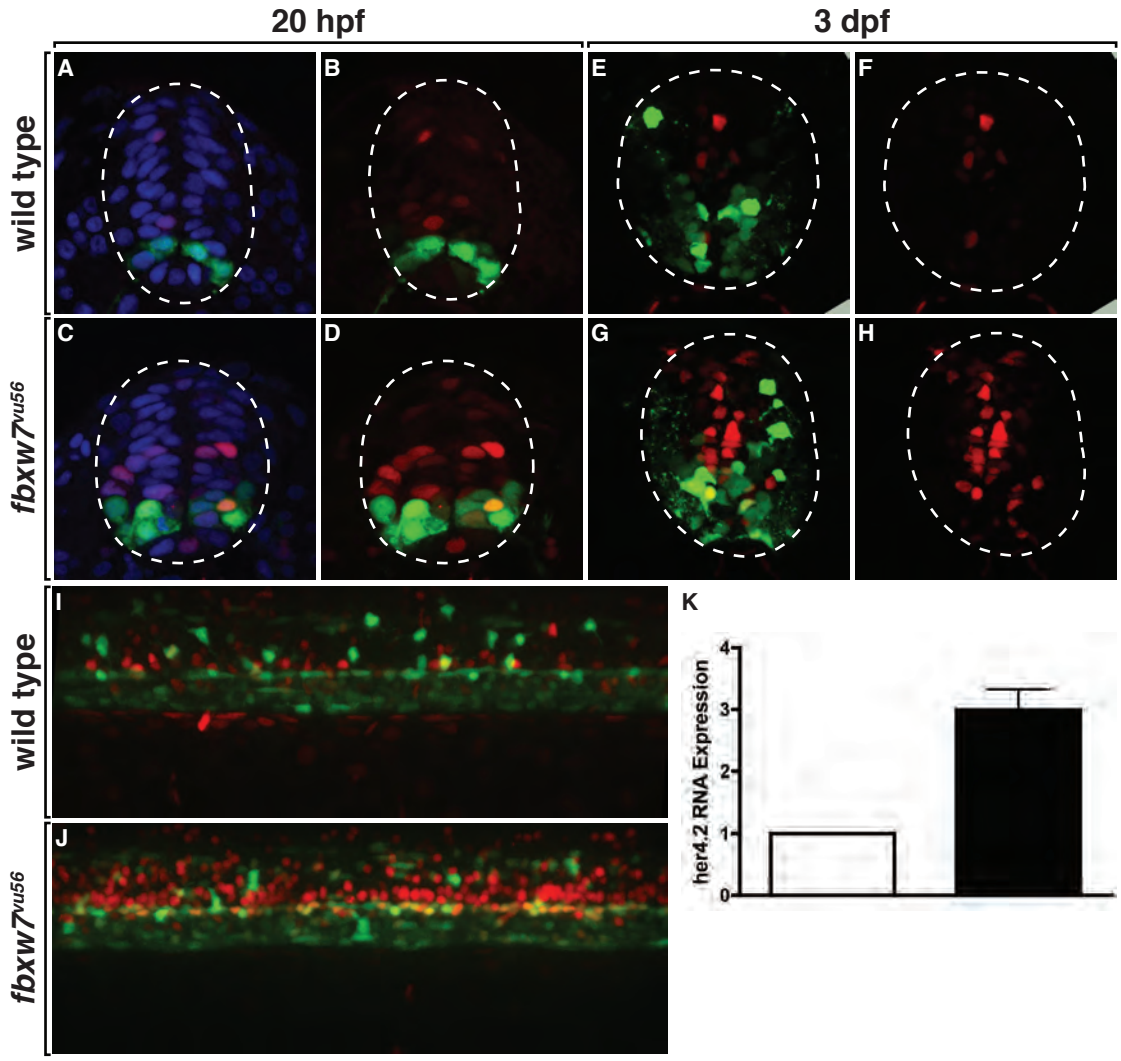

Figure 17 Notch activity in *fbxw7*^{vu56} mutants. **(A-H)** Transverse sections of 20 hpf **(A-D)** and 3 dpf **(E-H)** wild-type **(A,C)** and *fbxw7*^{vu56} mutant **(B,D)** spinal cords with Tg(*Tp1*:mCherry^{+}) and olig2:EGFP expression. Blue in **A,C** are DAPI labeled nuclei. **(I-J)** Lateral views of 6 dpf wild-type **(I)** and *fbxw7*^{vu56} mutant **(J)** spinal cords with Tg(*Tp1*:mCherry^{+}) and olig2:EGFP expression. **(K)** quantitative PCR of relative levels of her4.2 mRNA in 4dpf wild-type and *fbxw7*^{vu56} mutant larvae.

(Figure 17 K). The results of the previous two experiments are consistent with the hypothesis that Fbxw7 regulates Notch activity in the zebrafish nervous system.

Inhibition of Notch activity suppress the fbxw7$^{vu56-/-}$ phenotype

If the *fbxw7^{vu56}* excess OPC phenotype is a result of elevated Notch activity, suppression of the phenotype should occur with inhibition of Notch signaling. Embryos from crosses of Tg(*olig2:egfp*) heterozygous *fbxw7$^{vu56-/-}$* carriers were treated with γ-secretase inhibitor *N*-[*N*-(3,5-difluoro- phenacetyl-l-alanyl)]-*S*-phenylglycine *t*-butyl ester (DAPT) from 36 hpf, when OPCs begin to be specified, through 48 hpf, when OPCs begin to migrate, and assayed at 3 dpf for dorsal spinal cord OPCs. For each embryo, stereo and fluorescent images were acquired, followed by genotyping for the *fbxw7^{vu56}* mutation.

Previous experiments utilized high doses of DAPT, 100µM, which significantly impair Notch signaling. We wanted to see if a more subtle modulation of Notch activity with lower doses could alter activity enough to suppress the *fbxw7$^{vu56-/-}$* phenotype At a 25µM dose, embryos from all genotypes (*fbxw7$^{vu56+/+}$*, *fbxw7$^{vu56+/-}$*, and *fbxw7$^{vu56-/-}$*) had a normal morphology with a slight decrease in dorsal spinal cord OPCs compared to dimethyl sulfoxide (DMSO) control treated embryos (Figure 18 A-G). Increasing the dose to 50µM resulted in two classes of phenotypes in *fbxw7$^{vu56-/-}$* embryos: 25% had curved body and decreased OPCs, similar to sibling DAPT treated embryos (Figure (18K) while the remaining *fbxw7$^{vu56-/-}$* embryos had normal morphologies and approximately

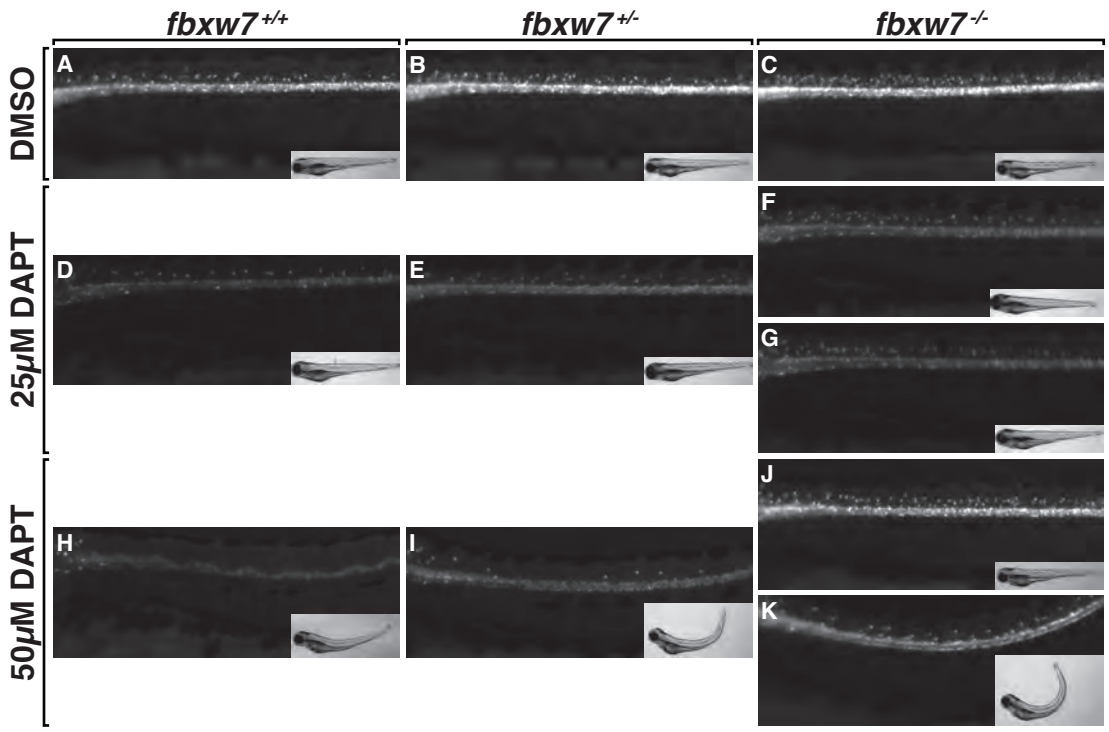

Figure 18 Modulation of Notch signaling suppress *fbxw7*^{vu56} phenotype. **(A-K)** Lateral images of 3 dpf *Tg*(*olig2:egfp*) larvae treated with DMSO or DAPT from 36-48 hpf. Insets show corresponding brightfield image of each larva. All larva were genotyped to determine zygousity.

the same number of OPCs (Figure 18J). These results indicate that inhibition of Notch signaling by DAPT suppresses the *fbxw7*$^{vu56-/-}$ excess OPC phenotype and supports our hypothesis that Fbxw7 regulates the active signaling amount of Notch proteins and limits specification of OPCs from neural precursors.

Discussion

Development of the spinal cord requires the specification and differentiation of many cells types. Oligodendrocytes are a glial cell responsible for the production of myelin sheaths that wrap axons. The number and distribution of oligodendrocytes must match to the number and distribution of axons. Previous experiments have demonstrated that forced expression of the ligand PDGF-AA in mice results in the formation of an excess number of OPCs early in development. However, these excess OPCs are removed by apoptosis and the mice have normal numbers of OPCs during post-natal development (Calver et al., 1998). Understanding the signaling pathways that control OPC number is important to be able to generate more OPCs when axons undergo demyelination due to either disease or injury.

Many signaling pathways are involved in oligodendrogenesis. The mechanisms by which those pathways are regulated are not well understood. Cells modulate the intensity and duration of signaling pathways through various methods. One method that affects the duration is protein degradation. Proteins are modified by the addition of ubiquitin moieties that are recognized by the proteasome.

Addition of ubiquitin occurs via several complexes, the first is the E1 ubiquitin-activating enzyme, the second is the E2 ubiquitin-conjugating enzyme, and then the E3 ubiquitin-ligase complex adds the ubiquitin to particular substrates based on the substrate specificity component of the complex. Fbxw7 is the substrate recognition component of the SCF (Skp-Cul-Fbox) E3 ubiquitin ligase complex. Several targets of Fbxw7 regulate the cell cycle including Cyclin E, c-Jun, and c-Myc as well as Notch signaling by targeting the NICD.

Notch signaling regulates the neuronal to glial fate switch. A role for Notch during neurogenesis came from studies in Drosophila investigating the induction of neuroblasts in the CNS (Artavantis-Tsakonas 1991) and sensory organ precursors (SOPs) in the PNS from ectoderm (Furukawa 1992, Schweisguth and Posakony 1992). Loss of function of Notch or overexpression of the ligands results in the formation of excess neurons at the expense of glia. Alternatively, overexpression of Notch inhibits neurogenesis and produces excess glia.

We investigated the mechanism by which *fbxw7*^{vu56} produced excess OPCs. Previously the lab discovered an increase of OPC number similar to the *fbxw7*^{vu56} phenotype using overexpression of the intracellular domain of Notch1a (Park and Appel, 2003). We hypothesized that misregulation of Notch was causing the excess OPC phenotype. Consistent with this hypothesis, modulation of Notch signaling with the chemical inhibitor DAPT, suppressed the excess OPC phenotype in *fbxw7*^{vu56} mutants.

Additionally, analysis of her4.2, a Notch target gene, by qPCR reveals an increase in Notch activity. A caveat for this experiment is that it is performed at 4

dpf, which is later than when the phenotype is first observed. However, because mutants cannot be identified prior to 3 dpf at the earliest, we are unable to analyze expression levels of Notch target genes during OPC specification by qPCR. A Notch transgenic reporter line *Tp1*:mcherry allows us to examine activity earlier as we can genotype embryos.

Overall, we show that Notch signaling is elevated in *fbxw7* mutant embryos and pharmacological inhibition of Notch signaling suppressed formation of excess OPCs indicating Notch proteins are functionally relevant targets of Fbxw7-mediated ubiquitination during oligodendrocyte specification. Our data provide evidence that negative regulation of Notch activity by protein degradation controls production of appropriate numbers of myelinating glial cells from neural precursors in vertebrate embryos.

CHAPTER VI

CONCLUSIONS

Understanding the development of the CNS is critical to learning how diseases and injuries alter the structure and function of the CNS in order to discover compounds that aid in regenerating and repairing insults. Specification of oligodendrocytes from neural precursors occurs at distinct times and places in the CNS. However, it is unclear how oligodendrocyte number is regulated, both during initial specification and as oligodendrocytes differentiate and contact axons. We sought to uncover novel mechanisms regulating oligodendrocyte number during development.

Regulation of OPC number by Fbxw7

Oligodendrocytes are produced from discrete locations within the CNS and migrate to populate the CNS. Specification in the spinal cord occurs in the ventral precursor domain pMN that also produces motor neurons. The mechanisms regulating the production of the proper number of neurons and oligodendrocytes from neural precursors are not clear.

We used the zebrafish spinal cord as a model system using a forward genetic screen to identify genes that are important for oligodendrocyte development. We isolated a mutation, *vu56*, which resulted in an excess number of OPCs at 3 dpf with no other obvious morphological phenotype both prior to and at this stage. Analysis of *vu56* identified *fbxw7* as the mutated gene. We

were able to demonstrate a role for Fbxw7 in regulating OPC number. Our results expand the understanding of the regulation of the number of OPCs from neural precursors.

Fbxw7 negatively regulates Notch in neural precursors

We also determined the mutation resulted in misregulation of Notch within pMN precursors to produce the excess OPCs. This is partially consistent with some conclusions from two recent investigations of mice with conditional knockout of Fbxw7 within the CNS using transgenic expression of Nestin-Cre (Hoeck et al., 2010; Matsumoto et al., 2011). Both groups reported a deficit of neurogenesis due to elevated Notch activity that blocked neuronal specification. However, Hoeck et al. also reported an increase in cell death due to elevated c-Jun, while Matsumoto et al. did not detect c-Jun elevation nor cell death. While Matsumoto et al. did detect an increase in the number of cells expressing the astrocyte marker GFAP, neither group found a change in oligodendrocyte number.

One possible explanation for the different effects of *Fbxw7* mutations in mice and zebrafish could be the presence of a second *fbxw7*-like gene in zebrafish. We did not find any evidence of a duplicated gene in the zebrafish genome. A second possibility is the relative oligodendrocyte number between mouse and zebrafish, the regions of the CNS examined, and the ability to directly observe oligodendrocytes. OPC number is regulated by several mechanisms including: amount of growth factors (Calver et al., 1998; van Heyningen et al.,

2001), cell-cell contact (Kirby et al., 2006), and cell density *in vitro* (Zhang and Miller, 1996). Therefore, the regions chosen for analysis may have precluded detection of changes in OPC number. A third possibility is the difference between misssense and null alleles. Because many of the Fbxw7 mutations in cancer are missense, Davis et al. (Davis et al., 2011) sought to determine if a missense allele would also produce different developmental defects. A mutation, R482Q, was introduced at a critical arginine residue. The R482Q mutation was perinatal lethal in the heterozygous state and homozygous mutants were lethal at E12.5. The heterozygous lethality was attributed to defects in lung development (Davis et al., 2011). Therefore, one might expect there to be different phenotypes associated with missense and null alleles of *fbxw7* in the spinal cord as well.

Additional experiments could be performed to further support the conclusion that Fbxw7 negatively regulates Notch in zebrafish. Studies from mouse, chick and zebrafish demonstrate that Notch activity in the ventral p2 domain determines the production V2a and V2b interneurons. Precursors in which Notch is active become V2b interneurons, while those in which Notch is inactive due to relatively higher Delta expression become V2a interneurons (Del Barrio et al., 2007; Kimura et al., 2008). V2 interneuron fate could be examined in *fbxw7*^{vu56} mutants using either *in situ* hybridization for *chx10* (V2a marker) or *gata2* (V2b marker) or antibodies commercially available or generated by Kimura et. al (Kimura et al., 2008). A caveat to these experiments would be the age of the embryos. The published results use timepoints between 16 hpf and 24 hpf, which is far earlier than when the excess OPC *fbxw7*^{vu56} phenotype can be

observed. One would likely need to image and genotype each embryo at the end of the experiment to determine if there is an effect.

Notch is also known to be important for retina development. The retina contains six neuronal and one glial cell types. Retinal neurons and glia are produced from progenitors along stereotypical waves during development (Cepko et al., 1996; Marquardt and Pfaff, 2001; Poggi et al., 2005a; 2005b). Notch activity is required to maintain a pool of progenitors available for the next wave of neurogenesis (Perron and Harris, 2000; Jadhav et al., 2006; Nelson et al., 2006). Recent research implicated interkinetic nuclear migration as a mechanism for regulating Notch activity of retinal progenitors (Del Bene et al., 2008). Preliminary experiments using a marker specific for the retinal ganglion cell layer showed defects in retina structure in *fbxw7*^{vu56} mutants. However, experiments of markers of other neuronal and glial cell types were inconclusive. Additional experiments could shed light on the apparent discrepancies.

Generation of a null allele of fbxw7 in zebrafish

An open question remains as to whether a null mutation of *fbxw7* in zebrafish would produce a different phenotype similar to differences observed in mouse (Davis et al., 2011) and in the variety of cancers with mutations of *fbxw7*. A study by Akhoondi et al. (Akhoondi et al., 2007) analyzed mutations of *FBXW7* in tumors of various origins including breast, colon, lung, bone, and others. Many of the *FBXW7* mutations were missense mutations at one of two Arg hotspots within the WD repeat that are responsible for substrate binding (Orlicky et al.,

2003; Hao et al., 2007). Another aspect to consider is the dimerization capacity of Fbxw7 (Welcker and Clurman, 2007). In addition to altering the binding of substrates, missense mutant forms of Fbxw7 could act as dominant-negatives to misregulate protein degradation (Akhoondi et al., 2007).

One difficulty with using zebrafish is specifically mutating a particular gene of interest. To analyze gene function, morpholinos are used to either inhibit translation or interfere with splicing to produce a null protein. Morpholinos do not always work for various reasons: a gene is maternally loaded in the egg and required for early development, the stage of development being investigated is later than the effective range of morpholinos, or blocking of translation or splicing is inefficient for unknown reasons. This technique also only produces null proteins.

There are now two techniques being used to generate null alleles of specific genes: Zinc-finger nucleases (ZFNs) and more recently TAL-effector nucleases (TALENs). Both function similarly in that they bind to DNA in a sequence specific manner. ZFNs are multimerized array zinc-finger DNA binding domains that each recognize a tri-nucleotide sequence fused to a FokI restriction enzyme domain (Bibikova et al., 2001; Miller et al., 2007). One problem with ZFNs is position-effect of the fingers whereby the relationship of each finger within the array affects efficacy (Amacher, 2008). TALENS are able to overcome this problem because each repeat within the TALEN recognizes a single nucleotide and there is no position-effect (Cermak et al., 2011; Li et al., 2011; Streubel et al., 2012). A recent report also used TALENs co-injected with DNA to

induce homologous recombination (Zu et al., 2013), which could be lead to ways to introduce a mutation within a gene or insert a reporter within an endogenous locus. The promise of these techniques should yield greater insight into development, including creating a null allele of *fbxw7* and comparing the results to *fbxw7*^{vu56}.

Phosphorylation of Notch is required for recognition by Fbxw7

Fbxw7 is known to target substrates based on phosphorylation of a specific amino acid sequence termed the Cdc4-phosphodegron (CPD) motif. Notch contains this CPD within the PEST region of the intracellular domain (Fryer et al., 2004; O'Neil et al., 2007). Several kinases are known to phosphorylate Notch, including Cdk8, GSK3β, and integrin-linked kinase (ILK) (Foltz et al., 2002; Fryer et al., 2004; O'Neil et al., 2007). What remains to be determined is if the kinases are expressed in neural precursors and whether they phosphorylate Notch *in vivo*.

Cdk8 phosphorylates a serine residue that lies at the +2 position within the predicted Notch CPD. Mutation of this residue leads to impaired phosphorylation and stabilization of NICD (Fryer et al., 2004). Additionally, mutation of the threonine within the CPD to alanine also stabilizes NICD (O'Neil et al., 2007).

Phosphorylation by ILK was demonstrated *in vitro* using tagged versions and mutants of ILK and Notch. ILK was required to phosphorylate NICD on Ser2173 within the transactivation domain (TAD), which is different from the CDK8 results. Mutation of other serine residue did not appear to affect NICD

stability by ILK (Mo et al., 2007). ILK is also a kinase upstream of GSK3β and regulation of Notch by ILK could be through a GSK3β mechanism. However, mutation of GSK3β to an inactive form that could not be phosphorylated did not alter the stability of NICD indicating regulation of NICD by ILK was independent of GSK3β (Mo et al., 2007).

While Mo et al. were able to show ILK phosphorylates NICD and affects stability via Fbxw7, the question remains if these are physiologically representative experiments (Mo et al., 2007). The serine residue is not located within the predicted Notch CPD and there could be other factors in the cell types used contributing to the observed phenotypes. More work needs to be done to determine if one of the already identified kinases plays a role in NICD stability in oligodendrocytes or if an unknown kinase is responsible. To that end, a search of Phosphonet (www.phosphonet.ca) predicts that ERK1, ERK or JNK2 could also phosphorylate NICD.

Differentiation of excess OPCs in fbxw7^{vu56} mutants

Excess OPCs persist in mutant *fbxw7$^{vu56-/-}$* larvae through at least 6 dpf. By this time oligodendrocytes have begun to start the process of wrapping axons. What remains unclear at this point is whether all the excess OPCs wrap axons and how this affects myelin formation. If the excess OPCs wrap axons, one might expect the internode lengths to be shorter due to more processes contacting axons that results in more nodes of Ranvier and decreased propagation of action potentials. Hypermyelination in mice by the overexpression of constitutively

active AKT did not affect oligodendrocyte number or survival and no physical abnormalities were reported (Flores et al., 2008; Narayanan et al., 2009). However, the mice died by 14 months (Flores et al., 2008).

Other targets of Fbxw7 during oligodendrocyte development

Our results indicate that the excess OPCs are able to undergo at least partial differentiation. This is inconsistent with previous reports that NICD activity plays an inhibitory role during oligodendrocyte differentiation (Wang et al., 1998). One way to reconcile the difference would be that another target of Fbxw7 is also disrupted that overrides the NICD activity. Indeed, activation of another target of Fbxw7, mammalian target of rapamycin (mTOR) (Mao et al., 2008) via Akt leads to hypermyelination in mice (Flores et al., 2008; Narayanan et al., 2009). mTOR is a protein kinase that associates with one of two complexes, mTORC1 or mTORC2. Upon activation by Akt, mTOR subsequently phosphorylates downstream targets to regulate translation, transcription, cell growth, and proliferation (reviewed in (Laplante and Sabatini, 2012)). Therefore, the continued differentiation of the excess OPCs could be explained by misregulated mTOR activity. A couple experiments could be proposed to investigate this hypothesis. First, similar to the modulation of Notch by DAPT, one could use rapamycin to modulate mTOR in *fbxw7* mutants to determine if differentiation of the excess OPCs is repressed and if the ectopic cells seen with *plp1a* expression are reduced or absent. Second, analysis of pathway activation could be

assessed by quantitative PCR (qPCR). Inhibition of mTOR in oligodendrocytes *in vitro* increased transcription of the target genes Id2, Id4, and Tcf4 (Tyler et al., 2009). Increased stability of mTOR could therefore lead to a decrease in the transcription of these target genes.

Identification of *fbxw7* as the gene disrupted in *vu56* provides a unique perspective on the regulation of OPC specification by Notch signaling. We show that regulation of Notch signaling by Fbxw7 is required within neural precursors to control OPC number. Our results reveal a novel mechanism regulating Notch signaling activity downstream of ligand activation in OPC specification. Further studies are needed to determine the kinase responsible for phosphorylating Notch in OPCs, the differentiation capacity of the excess OPCs, and what role, if any, other targets of Fbxw7 also play in oligodendrocyte development and differentiation.

REFERENCES

Akhoondi S et al. (2007) FBXW7/hCDC4 Is a General Tumor Suppressor in Human Cancer. Cancer Research 67:9006–9012.

Almeida AD, Wise HM, Hindley CJ, Slevin MK, Hartley RS, Philpott A (2010) The F-box protein Cdc4/Fbxw7 is a novel regulator of neural crest development in Xenopus laevis. Neural Dev 5:1.

Amacher SL (2008) Emerging gene knockout technology in zebrafish: zinc-finger nucleases. Briefings in Functional Genomics and Proteomics 7:460–464.

Andersson ER, Sandberg R, Lendahl U (2011) Notch signaling: simplicity in design, versatility in function. Development 138:3593–3612.

Appel B, Eisen JS (1998) Regulation of neuronal specification in the zebrafish spinal cord by Delta function. Development 125:371–380.

Appel B, Givan LA, Eisen JS (2001) Delta-Notch signaling and lateral inhibition in zebrafish spinal cord development. BMC Dev Biol 1:13.

Artavanis-Tsakonas S, Muskavitch MA, Yedvobnick B (1983) Molecular cloning of Notch, a locus affecting neurogenesis in Drosophila melanogaster. Proc Natl Acad Sci USA 80:1977–1981.

Artavanis-Tsakonas S, Rand MD, Lake RJ (1999) Notch signaling: cell fate control and signal integration in development. Science 284:770–776.

Austin JA, Kimble JE (1987) genetic and developmental analysis of glp-1. International C elegans Meeting.

Bahram F, Lehr von der N, Cetinkaya C, Larsson LG (2000) c-Myc hot spot mutations in lymphomas result in inefficient ubiquitination and decreased proteasome-mediated turnover. Blood 95:2104–2110.

Baron W, Shattil SJ, ffrench-Constant C (2002) The oligodendrocyte precursor mitogen PDGF stimulates proliferation by activation of alpha(v)beta3 integrins. EMBO J 21:1957–1966.

Barres BA, Raff MC (1994) Control of oligodendrocyte number in the developing rat optic nerve. Neuron 12:935–942.

Baumann N, Pham-Dinh D (2001) Biology of oligodendrocyte and myelin in the mammalian central nervous system. Physiol Rev 81:871–927.

Baumgart EV, Barbosa JS, Bally-Cuif L, Götz M, Ninkovic J (2012) Stab wound injury of the zebrafish telencephalon: a model for comparative analysis of reactive gliosis. Glia 60:343–357.

Bean BP (2007) The action potential in mammalian central neurons. Nat Rev Neurosci 8:451–465.

Bibikova M, Carroll D, Segal DJ, Trautman JK, Smith J, Kim YG, Chandrasegaran S (2001) Stimulation of Homologous Recombination through Targeted Cleavage by Chimeric Nucleases. Molecular and Cellular Biology 21:289–297.

Blakemore WF, Keirstead HS (1999) The origin of remyelinating cells in the central nervous system. Journal of Neuroimmunology 98:69–76.

Borggrefe T, Oswald F (2009) The Notch signaling pathway: transcriptional regulation at Notch target genes. Cell Mol Life Sci 66:1631–1646.

Br samle C, Halpern ME (2002) Characterization of myelination in the developing zebrafish. Glia 39:47–57.

Brady ST, Witt AS, Kirkpatrick LL, de Waegh SM, Readhead C, Tu PH, Lee VM (1999) Formation of compact myelin is required for maturation of the axonal cytoskeleton. Journal of Neuroscience 19:7278–7288.

Bray SJ (2006) Notch signalling: a simple pathway becomes complex. Nat Rev Mol Cell Biol 7:678–689.

Briscoe J, Pierani A, Jessell TM, Ericson J (2000) A homeodomain protein code specifies progenitor cell identity and neuronal fate in the ventral neural tube. Cell 101:435–445.

Briscoe J, Sussel L, Serup P, Hartigan-O'Connor D, Jessell TM, Rubenstein JL, Ericson J (1999) Homeobox gene Nkx2.2 and specification of neuronal identity by graded Sonic hedgehog signalling. Nature 398:622–627.

Bunge RP (1968) Glial cells and the central myelin sheath. Physiol Rev 48:197–251.

Cahoy JD, Emery B, Kaushal A, Foo LC, Zamanian JL, Christopherson KS, Xing Y, Lubischer JL, Krieg PA, Krupenko SA, Thompson WJ, Barres BA (2008) A transcriptome database for astrocytes, neurons, and oligodendrocytes: a new resource for understanding brain development and function. Journal of Neuroscience 28:264–278.

Cai J, Qi Y, Hu X, Tan M, Liu Z, Zhang J, Li Q, Sander M, Qiu M (2005) Generation of oligodendrocyte precursor cells from mouse dorsal spinal cord independent of Nkx6 regulation and Shh signaling. Neuron 45:41–53.

Calver AR, Hall AC, Yu WP, Walsh FS, Heath JK, Betsholtz C, Richardson WD (1998) Oligodendrocyte population dynamics and the role of PDGF in vivo. Neuron 20:869–882.

Castro B (2005) Lateral inhibition in proneural clusters: cis-regulatory logic and default repression by Suppressor of Hairless. Development 132:3333–3344.

Cepko CL, Austin CP, Yang X, Alexiades M, Ezzeddine D (1996) Cell fate determination in the vertebrate retina. Proc Natl Acad Sci USA 93:589–595.

Cermak T, Doyle EL, Christian M, Wang L, Zhang Y, Schmidt C, Baller JA, Somia NV, Bogdanove AJ, Voytas DF (2011) Efficient design and assembly of custom TALEN and other TAL effector-based constructs for DNA targeting. Nucleic Acids Res 39:e82.

Chiang C, Litingtung Y, Lee E, Young KE, Corden JL, Westphal H, Beachy PA (1996) Cyclopia and defective axial patterning in mice lacking Sonic hedgehog gene function. Nature 383:407–413.

Chitnis A, Henrique D, Lewis J, Ish-Horowicz D, Kintner C (1995) Primary neurogenesis in Xenopus embryos regulated by a homologue of the Drosophila neurogenic gene Delta. Nature 375:761–766.

Clarke JD, Holder N, Soffe SR, Storm-Mathisen J (1991) Neuroanatomical and functional analysis of neural tube formation in notochordless Xenopus embryos; laterality of the ventral spinal cord is lost. Development 112:499–516.

Coffman C, Harris W, Kintner C (1990) Xotch, the Xenopus homolog of Drosophila notch. Science 249:1438–1441.

Costello DJ, Eichler AF, Eichler FS (2009) Leukodystrophies: classification, diagnosis, and treatment. Neurologist 15:319–328.

Davis H, Lewis A, Spencer-Dene B, Tateossian H, Stamp G, Behrens A, Tomlinson I (2011) FBXW7 mutations typically found in human cancers are distinct from null alleles and disrupt lung development. J Pathol.

de la JLP, Wakeham A, Correia KM, Samper E, Brown S, Aguilera RJ, Nakano T, Honjo T, Mak TW, Rossant J, Conlon RA (1997) Conservation of the Notch signalling pathway in mammalian neurogenesis. ….

Del Barrio MG, Taveira-Marques R, Muroyama Y, Yuk DI, Li S, Wines-Samuelson M, Shen J, Smith HK, Xiang M, Rowitch D, Richardson WD (2007) A regulatory network involving Foxn4, Mash1 and delta-like 4/Notch1 generates V2a and V2b spinal interneurons from a common progenitor pool. Development 134:3427–3436.

Del Bene F, Wehman AM, Link BA, Baier H (2008) Regulation of Neurogenesis by Interkinetic Nuclear Migration through an Apical-Basal Notch Gradient. Cell 134:1055–1065.

Deneen B, Ho R, Lukaszewicz A, Hochstim CJ, Gronostajski RM, Anderson DJ (2006) The transcription factor NFIA controls the onset of gliogenesis in the developing spinal cord. Neuron 52:953–968.

Dexter JS (1914) The analysis of a case of continuous variation in Drosophila by a study of its linkage relations. American Naturalist.

Ebner S, Dunbar M, McKinnon RD (2000) Distinct roles for PI3K in proliferation and survival of oligodendrocyte progenitor cells. J Neurosci Res 62:336–345.

Echelard Y, Epstein DJ, St-Jacques B, Shen L, Mohler J, McMahon JA, McMahon AP (1993) Sonic hedgehog, a member of a family of putative signaling molecules, is implicated in the regulation of CNS polarity. Cell 75:1417–1430.

Emery B, Agalliu D, Cahoy JD, Watkins TA, Dugas JC, Mulinyawe SB, Ibrahim A, Ligon KL, Rowitch DH, Ben A Barres (2009) Myelin Gene Regulatory Factor Is a Critical Transcriptional Regulator Required for CNS Myelination. Cell 138:172–185.

Ericson J, Morton S, Kawakami A, Roelink H, Jessell TM (1996) Two critical periods of Sonic Hedgehog signaling required for the specification of motor neuron identity. Cell 87:661–673.

Fanarraga ML, Griffiths IR, McCulloch MC, Barrie JA, Kennedy PG, Brophy PJ (1992) Rumpshaker: an X-linked mutation causing hypomyelination: developmental differences in myelination and glial cells between the optic nerve and spinal cord. Glia 5:161–170.

Fang S, Weissman AM (2004) A field guide to ubiquitylation. Cell Mol Life Sci 61:1546–1561.

Finzsch M, Stolt CC, Lommes P, Wegner M (2008) Sox9 and Sox10 influence survival and migration of oligodendrocyte precursors in the spinal cord by regulating PDGF receptor alpha expression. Development 135:637–646.

Flores AI, Narayanan SP, Morse EN, Shick HE, Yin X, Kidd G, Avila RL, Kirschner DA, Macklin WB (2008) Constitutively active Akt induces enhanced myelination in the CNS. Journal of Neuroscience 28:7174–7183.

Fogarty M, Richardson WD, Kessaris N (2005) A subset of oligodendrocytes generated from radial glia in the dorsal spinal cord. Development 132:1951–1959.

Foltz DR, Santiago MC, Berechid BE, Nye JS (2002) Glycogen synthase kinase-3beta modulates notch signaling and stability. Curr Biol 12:1006–1011.Fortini ME (2002) Gamma-secretase-mediated proteolysis in cell-surface-receptor signalling. Nat Rev Mol Cell Biol 3:673–684.

Fortini ME (2009) Notch Signaling: The Core Pathway and Its Posttranslational Regulation. Developmental Cell 16:633–647.

Franklin R (1999) Review: Remyelination—A Regenerative Process in the CNS. The Neuroscientist.

Franklin RJM (2002) Why does remyelination fail in multiple sclerosis? Nat Rev Neurosci 3:705–714.

Frederick TJ, Wood TL (2004) IGF-I and FGF-2 coordinately enhance cyclin D1 and cyclin E–cdk2 association and activity to promote G1 progression in oligodendrocyte progenitor cells. Molecular and Cellular Neuroscience 25:480–492.

Fryer CJ, White JB, Jones KA (2004) Mastermind Recruits CycC:CDK8 to Phosphorylate the Notch ICD and Coordinate Activation with Turnover. Molecular Cell 16:509–520.

Gaiano N, Nye JS, Fishell G (2000) Radial glial identity is promoted by Notch1 signaling in the murine forebrain. Neuron 26:395–404.

Geisler R et al. (2007) Large-scale mapping of mutations affecting zebrafish development. BMC Genomics 8:11.

Glotzer M, Murray AW, Kirschner MW (1991) Cyclin is degraded by the ubiquitin pathway. Nature 349:132–138.

Gotoh H, Ono K, Takebayashi H, Harada H, Nakamura H, Ikenaka K (2011) Genetically-defined lineage tracing of Nkx2.2-expressing cells in chick spinal cord. Developmental Biology 349:504–511.

Greenwald I (1987) The lin-12 locus of Caenorhabditis elegans. Bioessays 6:70–73.

Greenwald IS, Sternberg PW, Horvitz HR (1983) The lin-12 locus specifies cell fates in Caenorhabditis elegans. Cell 34:435–444.

Gregory MA, Hann SR (2000) c-Myc proteolysis by the ubiquitin-proteasome pathway: stabilization of c-Myc in Burkitt's lymphoma cells. Molecular and Cellular Biology 20:2423–2435.

Gridley T (2010) Notch signaling in the vasculature. Curr Top Dev Biol 92:277–309.

Griffiths IR, Scott I, McCulloch MC, Barrie JA, McPhilemy K, Cattanach BM (1990) Rumpshaker mouse: a new X-linked mutation affecting myelination: evidence for a defect in PLP expression. J Neurocytol 19:273–283.

Gu Z, Inomata K, Ishizawa K, Horii A (2007) The FBXW7 beta-form is suppressed in human glioma cells. Biochemical and Biophysical Research Communications 354:992–998.

Gupta-Rossi N (2001) Functional Interaction between SEL-10, an F-box Protein, and the Nuclear Form of Activated Notch1 Receptor. Journal of Biological Chemistry 276:34371–34378.

Hao B, Oehlmann S, Sowa ME, Harper JW, Pavletich NP (2007) Structure of a Fbw7-Skp1-Cyclin E Complex: Multisite-Phosphorylated Substrate Recognition by SCF Ubiquitin Ligases. Molecular Cell 26:131–143.

Hauptmann G, Gerster T (2000) Multicolor whole-mount in situ hybridization. Methods Mol Biol 137:139–148.

Hereford LM, Hartwell LH (1974) Sequential gene function in the initiation of Saccharomyces cerevisiae DNA synthesis. J Mol Biol 84:445–461.

Hobson G, Garbern J (2012) Pelizaeus-Merzbacher Disease, Pelizaeus-Merzbacher-Like Disease 1, and Related Hypomyelinating Disorders. Semin Neurol 32:062–067.

Hoeck JD, Jandke A, Blake SM, Nye E, Spencer-Dene B, Brandner S, Behrens A (2010) Fbw7 controls neural stem cell differentiation and progenitor apoptosis via Notch and c-Jun. Nature Neuroscience:1–9.

Hubbard EJ, Wu G, Kitajewski J, Greenwald I (1997) sel-10, a negative regulator of lin-12 activity in Caenorhabditis elegans, encodes a member of the CDC4 family of proteins. Genes & Development 11:3182–3193.

Hueber SD, Lohmann I (2008) Shaping segments: Hox gene function in the genomic age. Bioessays 30:965–979.

Imayoshi I, Sakamoto M, Yamaguchi M, Mori K, Kageyama R (2010) Essential roles of Notch signaling in maintenance of neural stem cells in developing and adult brains. Journal of Neuroscience 30:3489–3498.

Irvine KD (1999) Fringe, Notch, and making developmental boundaries. Current Opinion in Genetics & Development 9:434–441.

Ishibashi T, Dakin KA, Stevens B, Lee PR, Kozlov SV, Stewart CL, Fields RD (2006) Astrocytes Promote Myelination in Response to Electrical Impulses. Neuron 49:823–832.

Itoh M, Kim C-H, Palardy G, Oda T, Jiang Y-J, Maust D, Yeo S-Y, Lorick K, Wright GJ, Ariza-McNaughton L, Weissman AM, Lewis J, Chandrasekharappa SC, Chitnis AB (2003) Mind bomb is a ubiquitin ligase that is essential for efficient activation of Notch signaling by Delta. Developmental Cell 4:67–82.

Jadhav AP, Cho S-H, Cepko CL (2006) Notch activity permits retinal cells to progress through multiple progenitor states and acquire a stem cell property. Proc Natl Acad Sci USA 103:18998–19003.

Jandke A, Da Costa C, Sancho R, Nye E, Spencer-Dene B, Behrens A (2011) The F-box protein Fbw7 is required for cerebellar development. Developmental Biology 358:201–212.

Jessell TM (2000) Neuronal specification in the spinal cord: inductive signals and transcriptional codes. Nat Rev Genet 1:20–29.

John GR, Shankar SL, Shafit-Zagardo B, Massimi A, Lee SC, Raine CS, Brosnan CF (2002) Multiple sclerosis: Re-expression of a developmental pathway that restricts oligodendrocyte maturation. Nat Med 8:1115–1121.

Kemp Z, Rowan A, Chambers W, Wortham N, Halford S, Sieber O, Mortensen N, Herbay von A, Gunther T, Ilyas M, Tomlinson I (2005) CDC4 mutations occur in a subset of colorectal cancers but are not predicted to cause loss of function and are not associated with chromosomal instability. Cancer Research 65:11361–11366.

Kessaris N, Fogarty M, Iannarelli P, Grist M, Wegner M, Richardson WD (2006) Competing waves of oligodendrocytes in the forebrain and postnatal elimination of an embryonic lineage. Nature Neuroscience 9:173–179.

Kidd S, Lockett TJ, Young MW (1983) The Notch locus of Drosophila melanogaster. Cell 34:421–433.

Kimmel CB, Ballard WW, Kimmel SR, Ullmann B, Schilling TF (1995) Stages of embryonic development of the zebrafish. Dev Dyn 203:253–310.

Kimura Y, Satou C, Higashijima SI (2008) V2a and V2b neurons are generated by the final divisions of pair-producing progenitors in the zebrafish spinal cord. Development 135:3001–3005.

Kirby BB, Takada N, Latimer AJ, Shin J, Carney TJ, Kelsh RN, Appel B (2006) In vivo time-lapse imaging shows dynamic oligodendrocyte progenitor behavior during zebrafish development. Nature Neuroscience 9:1506–1511.

Kuhlbrodt K, Herbarth B, Sock E, Enderich J, Hermans-Borgmeyer I, Wegner M (1998) Cooperative function of POU proteins and SOX proteins in glial cells. J Biol Chem 273:16050–16057.

Kuhlmann T, Miron V, Cui Q, Cuo Q, Wegner C, Antel J, Brück W (2008) Differentiation block of oligodendroglial progenitor cells as a cause for remyelination failure in chronic multiple sclerosis. Brain 131:1749–1758.

Laplante M, Sabatini DM (2012) mTOR signaling in growth control and disease. Cell 149:274–293.

Lee JE, Hollenberg SM, Snider L, Turner DL, Lipnick N (1995) Conversion of Xenopus ectoderm into neurons by NeuroD, a basic helix-loop-helix protein. Science.

Lee JW, Soung YH, Kim HJ, Park WS, Nam SW, Kim SH, Lee JY, Yoo NJ, Lee SH (2006) Mutational analysis of the hCDC4 gene in gastric carcinomas. Eur J Cancer 42:2369–2373.

Li H, Lu Y, Smith HK, Richardson WD (2007) Olig1 and Sox10 interact synergistically to drive myelin basic protein transcription in oligodendrocytes. Journal of Neuroscience 27:14375–14382.

Li T, Huang S, Zhao X, Wright DA, Carpenter S, Spalding MH, Weeks DP, Yang B (2011) Modularly assembled designer TAL effector nucleases for targeted gene knockout and gene replacement in eukaryotes. Nucleic Acids Res 39:6315–6325.

Liu L, Chong S-W, Balasubramaniyan NV, Korzh V, Ge R (2002a) Platelet-derived growth factor receptor alpha (pdgfr-alpha) gene in zebrafish embryonic development. Mechanisms of Development 116:227–230.

Liu L, Korzh V, Balasubramaniyan N, Ekker M, Ge R (2002b) Platelet-derived growth factor A (pdgf-a) expression during zebrafish embryonic development. Dev Genes Evol 212:298–301.

Liu Z, Hu X, Cai J, Liu B, Peng X, Wegner M, Qiu M (2007) Induction of oligodendrocyte differentiation by Olig2 and Sox10: Evidence for reciprocal interactions and dosage-dependent mechanisms. Developmental Biology 302:683–693.

Lu QR, Sun T, Zhu Z, Ma N, Garcia M, Stiles CD, Rowitch DH (2002) Common developmental requirement for Olig function indicates a motor neuron/oligodendrocyte connection. Cell 109:75–86.

Lu QR, Yuk D, Alberta JA, Zhu Z, Pawlitzky I, Chan J, McMahon AP, Stiles CD, Rowitch DH (2000) Sonic hedgehog--regulated oligodendrocyte lineage genes encoding bHLH proteins in the mammalian central nervous system. Neuron 25:317–329.

Lucchinetti CF, Parisi J, Bruck W (2005) The pathology of multiple sclerosis. Neurologic Clinics 23:77–105.

Lütolf S, Radtke F, Aguet M, Suter U, Taylor V (2002) Notch1 is required for neuronal and glial differentiation in the cerebellum. Development 129:373–385.

Lyon G, Fattal-Valevski A, Kolodny EH (2006) Leukodystrophies: clinical and genetic aspects. Top Magn Reson Imaging 17:219–242.

Ma Q, Kintner C, Anderson DJ (1996) Identification of neurogenin, a Vertebrate Neuronal Determination Gene. Cell.

Maier CE, Miller RH (1995) Development of glial cytoarchitecture in the frog spinal cord. Dev Neurosci 17:149–159.

Mao J-H, Perez-Losada J, Wu D, Delrosario R, Tsunematsu R, Nakayama KI, Brown K, Bryson S, Balmain A (2004) Fbxw7/Cdc4 is a p53-dependent, haploinsufficient tumour suppressor gene. Nature 432:775–779.

Mao JH, Kim IJ, Wu D, Climent J, Kang HC, DelRosario R, Balmain A (2008) FBXW7 Targets mTOR for Degradation and Cooperates with PTEN in Tumor Suppression. Science 321:1499–1502.

Marquardt T, Pfaff SL (2001) Cracking the transcriptional code for cell specification in the neural tube. Cell 106:651–654.

Maruyama S (2001) Characterization of a Mouse Gene (Fbxw6) That Encodes a Homologue of Caenorhabditis elegans SEL-10. Genomics 78:214–222.

Matsumoto A, Onoyama I, Nakayama KI (2006) Expression of mouse Fbxw7 isoforms is regulated in a cell cycle- or p53-dependent manner. Biochemical and Biophysical Research Communications 350:114–119.

Matsumoto S, Onoyama I, Sunabori T, Kageyama R, Okano H, Nakayama KI (2011) Fbxw7-dependent Degradation of Notch Is Required for Control of “Stemness” and Neuronal-Glial Differentiation in Neural Stem Cells. Journal of Biological Chemistry 286:13754–13764.

Matsuoka S et al. (2008) Fbxw7 acts as a critical fail-safe against premature loss of hematopoietic stem cells and development of T-ALL. Genes & Development 22:986–991.

McKinnon RD, Matsui T, Dubois-Dalcq M, Aaronson SA (1990) FGF modulates the PDGF-driven pathway of oligodendrocyte development. Neuron 5:603–614.

McMorris FA, McKinnon RD (1996) Regulation of oligodendrocyte development and CNS myelination by growth factors: prospects for therapy of demyelinating disease. Brain Pathol 6:313–329.

Michailov GV, Sereda MW, Brinkmann BG, Fischer TM, Haug B, Birchmeier C, Role L, Lai C, Schwab MH, Nave K-A (2004) Axonal neuregulin-1 regulates myelin sheath thickness. Science 304:700–703.

Miller AC, Lyons EL, Herman TG (2009) cis-Inhibition of Notch by endogenous Delta biases the outcome of lateral inhibition. Curr Biol 19:1378–1383.

Miller JC, Holmes MC, Wang J, Guschin DY, Lee Y-L, Rupniewski I, Beausejour CM, Waite AJ, Wang NS, Kim KA, Gregory PD, Pabo CO, Rebar EJ (2007) An improved zinc-finger nuclease architecture for highly specific genome editing. Nature Biotechnology 25:778–785.

Miller RH, Payne J, Milner L, Zhang H, Orentas DM (1997) Spinal cord oligodendrocytes develop from a limited number of migratory highly proliferative precursors. J Neurosci Res 50:157–168.

Mo JS, Kim MY, Han SO, Kim IS, Ann EJ, Lee KS, Seo MS, Kim JY, Lee SC, Park JW, Choi EJ, Seong JY, Joe CO, Faessler R, Park HS (2007) Integrin-Linked Kinase Controls Notch1 Signaling by Down-Regulation of Protein Stability through Fbw7 Ubiquitin Ligase. Molecular and Cellular Biology 27:5565–5574.

Mohr OL (1919) Character Changes Caused by Mutation of an Entire Region of a Chromosome in Drosophila. Genetics 4:275–282.

Nakayama KI, Nakayama K (2006) Ubiquitin ligases: cell-cycle control and cancer. Nat Rev Cancer 6:369–381.

Narayanan SP, Flores AI, Wang F, Macklin WB (2009) Akt signals through the mammalian target of rapamycin pathway to regulate CNS myelination. Journal of Neuroscience 29:6860–6870.

Nash P, Tang X, Orlicky S, Chen Q, Gertler FB, Mendenhall MD, Sicheri F, Pawson T, Tyers M (2001) Multisite phosphorylation of a CDK inhibitor sets a threshold for the onset of DNA replication. Nature 414:514–521.

Nelson BR, Gumuscu B, Hartman BH, Reh TA (2006) Notch Activity Is Downregulated Just prior to Retinal Ganglion Cell Differentiation. Dev Neurosci 28:128–141.

Neve LD, Savage AA, Koke JR, García DM (2012) Activating transcription factor 3 and reactive astrocytes following optic nerve injury in zebrafish. Comp Biochem Physiol C Toxicol Pharmacol 155:213–218.

Ng PC, Henikoff S (2001) Predicting deleterious amino acid substitutions. Genome Research 11:863–874.

Nicholson SC, Gilbert MM, Nicolay BN, Frolov MV, Moberg KH (2009) The archipelago tumor suppressor gene limits rb/e2f-regulated apoptosis in developing Drosophila tissues. Curr Biol 19:1503–1510.

Niwa Y, Shimojo H, Isomura A, González A, Miyachi H, Kageyama R (2011) Different types of oscillations in Notch and Fgf signaling regulate the spatiotemporal periodicity of somitogenesis. Genes & Development 25:1115–1120.

Novitch BG, Chen AI, Jessell TM (2001) Coordinate regulation of motor neuron subtype identity and pan-neuronal properties by the bHLH repressor Olig2. Neuron 31:773–789.

O'Neil J, Grim J, Strack P, Rao S, Tibbitts D, Winter C, Hardwick J, Welcker M, Meijerink JP, Pieters R, Draetta G, Sears R, Clurman BE, Look AT (2007) FBW7 mutations in leukemic cells mediate NOTCH pathway activation and resistance to -secretase inhibitors. Journal of Experimental Medicine 204:1813–1824.

Oberg C (2001) The Notch Intracellular Domain Is Ubiquitinated and Negatively Regulated by the Mammalian Sel-10 Homolog. Journal of Biological Chemistry 276:35847–35853.

Oginuma M, Takahashi Y, Kitajima S, Kiso M, Kanno J, Kimura A, Saga Y (2010) The oscillation of Notch activation, but not its boundary, is required for somite border formation and rostral-caudal patterning within a somite. Development 137:1515–1522.

ONO K, BANSAL R, Payne J, Rutishauser U, Miller RH (1995) Early development and dispersal of oligodendrocyte precursors in the embryonic chick spinal cord. Development 121:1743–1754.

Orentas DM, Hayes JE, Dyer KL, Miller RH (1999) Sonic hedgehog signaling is required during the appearance of spinal cord oligodendrocyte precursors. Development 126:2419–2429.

Orlicky S, Tang X, Willems A, Tyers M, Sicheri F (2003) Structural basis for phosphodependent substrate selection and orientation by the SCFCdc4 ubiquitin ligase. Cell 112:243–256.

Park H-C, Appel B (2003) Delta-Notch signaling regulates oligodendrocyte specification. Development 130:3747–3755.

Park H-C, Boyce J, Shin J, Appel B (2005) Oligodendrocyte specification in zebrafish requires notch-regulated cyclin-dependent kinase inhibitor function. Journal of Neuroscience 25:6836–6844.

Park H-C, Mehta A, Richardson JS, Appel B (2002) olig2 is required for zebrafish primary motor neuron and oligodendrocyte development. Developmental Biology 248:356–368.

Parpura V, Heneka MT, Montana V, Oliet SHR, Schousboe A, Haydon PG, Stout RF, Spray DC, Reichenbach A, Pannicke T, Pekny M, Pekna M, Zorec R, Verkhratsky A (2012) Glial cells in (patho)physiology. J Neurochem 121:4–27.

Parsons MJ, Pisharath H, Yusuff S, Moore JC, Siekmann AF, Lawson N, Leach SD (2009) Notch-responsive cells initiate the secondary transition in larval zebrafish pancreas. Mechanisms of Development:1–15.

Pastores GM (2009) Krabbe disease: an overview. Int J Clin Pharmacol Ther 47 Suppl 1:S75–S81.

Perlman SJ, Mar S (2012) Leukodystrophies. Adv Exp Med Biol 724:154–171.

Perron M, Harris WA (2000) Determination of vertebrate retinal progenitor cell fate by the Notch pathway and basic helix-loop-helix transcription factors. Cell Mol Life Sci 57:215–223.

Peters J-M (2006) The anaphase promoting complex/cyclosome: a machine designed to destroy. Nat Rev Mol Cell Biol 7:644–656.

Pfeiffer SE, Warrington AE, BANSAL R (1993) The oligodendrocyte and its many cellular processes. Trends Cell Biol 3:191–197.

Poggi L, Vitorino M, Masai I, Harris WA (2005a) Influences on neural lineage and mode of division in the zebrafish retina in vivo. The Journal of Cell Biology 171:991–999.

Poggi L, Zolessi FR, Harris WA (2005b) Time-lapse analysis of retinal differentiation. Curr Opin Cell Biol 17:676–681.

Popov N, Wanzel M, Madiredjo M, Zhang D, Beijersbergen R, Bernards R, Moll R, Elledge SJ, Eilers M (2007) The ubiquitin-specific protease USP28 is required for MYC stability. Nat Cell Biol 9:765–774.

Postlethwait JH, Talbot WS (1997) Zebrafish genomics: from mutants to genes. Trends Genet 13:183–190.

Priess JR, Schnabel H, Schnabel R (1987) The glp-1 locus and cellular interactions in early C. elegans embryos. Cell 51:601–611.

Pringle NP, Richardson WD (1993) A singularity of PDGF alpha-receptor expression in the dorsoventral axis of the neural tube may define the origin of the oligodendrocyte lineage. Development 117:525–533.

Prinz M, Priller J, Sisodia SS, Ransohoff RM (2011) Heterogeneity of CNS myeloid cells and their roles in neurodegeneration. Nature Neuroscience 14:1227–1235.

Rabadán MA, Cayuso J, Le Dréau G, Cruz C, Barzi M, Pons S, Briscoe J, Martí E (2012) Jagged2 controls the generation of motor neuron and oligodendrocyte progenitors in the ventral spinal cord. Cell Death Differ 19:209–219.

Raff MC, Lillien LE, Richardson WD, Burne JF, Noble MD (1988) Platelet-derived growth factor from astrocytes drives the clock that times oligodendrocyte development in culture. Nature 333:562–565.

Ramensky V, Bork P, Sunyaev S (2002) Human non-synonymous SNPs: server and survey. Nucleic Acids Res 30:3894–3900.

Richardson WD, Kessaris N, Pringle N (2006) Oligodendrocyte wars. Nat Rev Neurosci 7:11–18.

Richardson WD, Smith HK, Sun T, Pringle NP, Hall A, Woodruff R (2000) Oligodendrocyte lineage and the motor neuron connection. Glia 29:136–142.

Roelink H, Augsburger A, Heemskerk J, Korzh V, Norlin S, Ruiz i Altaba A, Tanabe Y, Placzek M, Edlund T, Jessell TM (1994) Floor plate and motor neuron induction by vhh-1, a vertebrate homolog of hedgehog expressed by the notochord. Cell 76:761–775.

Roelink H, Porter JA, Chiang C, Tanabe Y, Chang DT, Beachy PA, Jessell TM (1995) Floor plate and motor neuron induction by different concentrations of the amino-terminal cleavage product of sonic hedgehog autoproteolysis. Cell 81:445–455.

Rowitch DH (2004) Glial specification in the vertebrate neural tube. Nat Rev Neurosci 5:409–419.

Rowitch DH, Kriegstein AR (2010) Developmental genetics of vertebrate glial-cell specification. Nature 468:214–222.

Saijo K, Glass CK (2011) Microglial cell origin and phenotypes in health and disease. Nat Rev Immunol 11:775–787.

Salzer JL, Brophy PJ, Peles E (2008) Molecular domains of myelinated axons in the peripheral nervous system. Glia 56:1532–1540.

Schroeter EH, Kisslinger JA, Kopan R (1998) Notch-1 signalling requires ligand-induced proteolytic release of intracellular domain. Nature 393:382–386.

Selkoe D, Kopan R (2003) Notch and Presenilin: regulated intramembrane proteolysis links development and degeneration. Annu Rev Neurosci 26:565–597.

Sherman DL, Brophy PJ (2005) Mechanisms of axon ensheathment and myelin growth. Nat Rev Neurosci 6:683–690.

Shimoda N, Knapik EW, Ziniti J, Sim C, Yamada E, Kaplan S, Jackson D, de Sauvage F, Jacob H, Fishman MC (1999) Zebrafish genetic map with 2000 microsatellite markers. Genomics 58:219–232.

Shin J, Park H-C, Topczewska JM, Mawdsley DJ, Appel B (2003) Neural cell fate analysis in zebrafish using olig2 BAC transgenics. Methods Cell Sci 25:7–14.

Shin J, Poling J, Park HC, Appel B (2007) Notch signaling regulates neural precursor allocation and binary neuronal fate decisions in zebrafish. Development 134:1911–1920.

Solnica-Krezel L, Schier AF, Driever W (1994) Efficient recovery of ENU-induced mutations from the zebrafish germline. Genetics 136:1401–1420.

Sommer L, Ma Q, Anderson DJ (1996) neurogenins, a Novel Family of atonal-Related bHLH Transcription Factors, Are Putative Mammalian Neuronal Determination Genes That Reveal …. Molecular and Cellular Neuroscience.

Sprinzak D, Lakhanpal A, LeBon L, Santat LA, Fontes ME, Anderson GA, Garcia-Ojalvo J, Elowitz MB (2010) Cis-interactions between Notch and Delta generate mutually exclusive signalling states. Nature 465:86–90.

Spruck CH, Strohmaier H, Sangfelt O, Müller HM, Hubalek M, Müller-Holzner E, Marth C, Widschwendter M, Reed SI (2002) hCDC4 gene mutations in endometrial cancer. Cancer Research 62:4535–4539.

Stolt CC (2002) Terminal differentiation of myelin-forming oligodendrocytes depends on the transcription factor Sox10. Genes & Development 16:165–170.

Stolt CC, Lommes P, Sock E, Chaboissier M-C, Schedl A, Wegner M (2003) The Sox9 transcription factor determines glial fate choice in the developing spinal cord. Genes & Development 17:1677–1689.

Streubel J, Blücher C, Landgraf A, Boch J (2012) TAL effector RVD specificities and efficiencies. Nature Biotechnology 30:593–595.

Strohmaier H, Spruck CH, Kaiser P, Won KA, Sangfelt O, Reed SI (2001) Human F-box protein hCdc4 targets cyclin E for proteolysis and is mutated in a breast cancer cell line. Nature 413:316–322.

Takada N, Appel B (2010) Identification of genes expressed by zebrafish oligodendrocytes using a differential microarray screen. Dev Dyn 239:2041–2047.

Takada N, Kucenas S, Appel B (2010) Sox10 is necessary for oligodendrocyte survival following axon wrapping. Glia:NA–NA.

Takebayashi H, Ohtsuki T, Uchida T, Kawamoto S, Okubo K, Ikenaka K, Takeichi M, Chisaka O, Nabeshima Y-I (2002) Non-overlapping expression of Olig3 and Olig2 in the embryonic neural tube. Mechanisms of Development 113:169–174.

Takebayashi H, Yoshida S, Sugimori M, Kosako H, Kominami R, Nakafuku M, Nabeshima Y (2000) Dynamic expression of basic helix-loop-helix Olig family members: implication of Olig2 in neuron and oligodendrocyte differentiation and identification of a new member, Olig3. Mechanisms of Development 99:143–148.

Tan Y, Sangfelt O, Spruck C (2008) The Fbxw7/hCdc4 tumor suppressor in human cancer. Cancer Letters 271:1–12.

Tanabe Y, Jessell TM (1996) Diversity and pattern in the developing spinal cord. Science 274:1115–1123.

Tanigaki K, Nogaki F, Takahashi J, Tashiro K, Kurooka H, Honjo T (2001) Notch1 and Notch3 instructively restrict bFGF-responsive multipotent neural progenitor cells to an astroglial fate. Neuron 29:45–55.

Taylor MK, Yeager K, Morrison SJ (2007) Physiological Notch signaling promotes gliogenesis in the developing peripheral and central nervous systems. Development 134:2435–2447.

Tetzlaff MT, Yu W, Li M, Zhang P, Finegold M, Mahon K, Harper JW, Schwartz RJ, Elledge SJ (2004) Defective cardiovascular development and elevated cyclin E and Notch proteins in mice lacking the Fbw7 F-box protein. Proc Natl Acad Sci USA 101:3338–3345.

Thomas GB, van Meyel DJ (2006) The glycosyltransferase Fringe promotes Delta-Notch signaling between neurons and glia, and is required for subtype-specific glial gene expression. Development 134:591–600.

Thompson BJ, Buonamici S, Sulis ML, Palomero T, Vilimas T, Basso G, Ferrando A, Aifantis I (2007) The SCFFBW7 ubiquitin ligase complex as a tumor suppressor in T cell leukemia. J Exp Med 204:1825–1835.

Tsakonas SA, Grimwade BG (1983) The Notch locus of Drosophila melanogaster: A molecular analysis. Developmental ….

Tsunematsu R (2004) Mouse Fbw7/Sel-10/Cdc4 Is Required for Notch Degradation during Vascular Development. Journal of Biological Chemistry 279:9417–9423.

Tümpel S, Wiedemann LM, Krumlauf R (2009) Hox genes and segmentation of the vertebrate hindbrain. Curr Top Dev Biol 88:103–137.

Tyler WA, Gangoli N, Gokina P, Kim HA, Covey M, Levison SW, Wood TL (2009) Activation of the mammalian target of rapamycin (mTOR) is essential for oligodendrocyte differentiation. Journal of Neuroscience 29:6367–6378.

Vallstedt A, Klos JM, Ericson J (2005) Multiple dorsoventral origins of oligodendrocyte generation in the spinal cord and hindbrain. Neuron 45:55–67.

van Heyningen P, Calver AR, Richardson WD (2001) Control of progenitor cell number by mitogen supply and demand. Curr Biol 11:232–241.

van Straaten HW, Hekking JW, Wiertz-Hoessels EJ, Thors F, Drukker J (1988) Effect of the notochord on the differentiation of a floor plate area in the neural tube of the chick embryo. Anat Embryol 177:317–324.

van Tetering G, van Diest P, Verlaan I, van der Wall E, Kopan R, Vooijs M (2009) Metalloprotease ADAM10 is required for Notch1 site 2 cleavage. Journal of Biological Chemistry 284:31018–31027.

Wang S, Sdrulla AD, diSibio G, Bush G, Nofziger D, Hicks C, Weinmaster G, Barres BA (1998) Notch receptor activation inhibits oligodendrocyte differentiation. Neuron 21:63–75.

Warf BC, Fok-Seang J, Miller RH (1991) Evidence for the ventral origin of oligodendrocyte precursors in the rat spinal cord. J Neurosci 11:2477–2488.

Wegner M, Stolt CC (2005) From stem cells to neurons and glia: a Soxist's view of neural development. Trends in Neurosciences 28:583–588.

Welcker M, Clurman BE (2007) Fbw7/hCDC4 dimerization regulates its substrate interactions. Cell Div 2:7.

Welcker M, Clurman BE (2008) FBW7 ubiquitin ligase: a tumour suppressor at the crossroads of cell division, growth and differentiation. Nat Rev Cancer 8:83–93.

Welcker M, Orian A, Grim JA, Eisenman RN, Clurman BE (2004) A Nucleolar Isoform of the Fbw7 Ubiquitin Ligase Regulates c-Myc and Cell Size. Current Biology 14:1852–1857.

Wen C, Metzstein MM, Greenwald I (1997) SUP-17, a Caenorhabditis elegans ADAM protein related to Drosophila KUZBANIAN, and its role in LIN-12/NOTCH signalling. Development 124:4759–4767.

Weng AP, Ferrando AA, Lee W, Morris JP, Silverman LB, Sanchez-Irizarry C, Blacklow SC, Look AT, Aster JC (2004) Activating mutations of NOTCH1 in human T cell acute lymphoblastic leukemia. Science 306:269–271.

Wolswijk G (2000) Oligodendrocyte survival, loss and birth in lesions of chronic-stage multiple sclerosis. Brain 123 (Pt 1):105–115.

Wolswijk G (2002) Oligodendrocyte precursor cells in the demyelinated multiple sclerosis spinal cord. Brain 125:338–349.

Wood PM, Bunge RP (1991) The origin of remyelinating cells in the adult central nervous system: the role of the mature oligodendrocyte. Glia 4:225–232.

Wu G, Lyapina S, Das I, Li J, Gurney M, Pauley A, Chui I, Deshaies RJ, Kitajewski J (2001) SEL-10 is an inhibitor of notch signaling that targets notch for ubiquitin-mediated protein degradation. Molecular and Cellular Biology 21:7403–7415.

Yada M, Hatakeyama S, Kamura T, Nishiyama M, Tsunematsu R, Imaki H, Ishida N, Okumura F, Nakayama K, Nakayama KI (2004) Phosphorylation-dependent degradation of c-Myc is mediated by the F-box protein Fbw7. EMBO J 23:2116–2125.

Yamada T, Placzek M, Tanaka H, Dodd J, Jessell TM (1991) Control of cell pattern in the developing nervous system: polarizing activity of the floor plate and notochord. Cell 64:635–647.

Yang X, Tomita T, Wines-Samuelson M, Beglopoulos V, Tansey MUG, Kopan R, Shen J (2006) Notch1 Signaling Influences V2 Interneuron and Motor Neuron Development in the Spinal Cord. Dev Neurosci 28:102–117.

Zhang H, Miller RH (1996) Density-dependent feedback inhibition of oligodendrocyte precursor expansion. J Neurosci 16:6886–6895.

Zhou Q, Anderson DJ (2002) The bHLH transcription factors OLIG2 and OLIG1 couple neuronal and glial subtype specification. Cell 109:61–73.

Zhou Q, Choi G, Anderson DJ (2001) The bHLH transcription factor Olig2 promotes oligodendrocyte differentiation in collaboration with Nkx2.2. Neuron 31:791–807.

Zhou Q, Wang S, Anderson DJ (2000) Identification of a novel family of oligodendrocyte lineage-specific basic helix-loop-helix transcription factors. Neuron 25:331–343.

Zu Y, Tong X, Wang Z, Liu D, Pan R, Li Z, Hu Y, Luo Z, Huang P, Wu Q, Zhu Z, Zhang B, Lin S (2013) TALEN-mediated precise genome modification by homologous recombination in zebrafish. Nat Meth.